공학박사학위논문

Development of carbon nanotube-based bioelectronic sensors using receptor proteins and peptides for to water and food quality assessment and disease diagnosis

수용체 단백질과 펩타이드를 이용한 탄소나노튜브 기반의 바이오전자 센서 개발 및 수질과 음식물 품질평가 및 질병진단으로의 응용

2016 년 8 월

서울대학교 대학원

공과대학 협동과정 바이오엔지니어링

손 만 기

Abstract

Development of carbon nanotube-based bioelectronic sensors using receptor proteins and peptides for water and food quality assessment and disease diagnosis

Manki Son

Interdisciplinary Program for Bioengineering

The Graduate School

Seoul National University

Bioelectronic sensors that combine biomolecules as primary recognition elements and electronics as signal transducers have been extensively developed.[1, 2] Biologically-inspired technologies for detection of target molecules increased the functionality of sensors with the nature system. Nanomaterial-based electronic devices rapidly amplify biological signals and convert into intuitive forms.[3, 4, 5] Furthermore, many parts of living organisms are operated by action potentials so that they can be applied to the sensing mechanism of biolectronic sensors. Recently, various nanomaterials, such as carbon nanotube (CNT), graphene, nanoparticle, nanofiber, nanowire and nanofilm have been used in the fabrication of the bioelectronic sensors. Such nanomaterials were functionalized with biomolecules, such as DNA, protein, peptide, and cell for the specific binding. Advantages of using bioelectronic sensors are low manufacturing cost, small size, fast response, high sensitivity

and selectivity.

The objective of this research is to develop a CNT-based bioelectronic sensor using receptor proteins and peptides for various applications. Receptors receive external stimuli from out of the cell membrane and activate signal transduction pathways.[6] The Receptors play important functions in the human body such as sensory transduction, cellular communication, neural transmission and hormonal signaling.[7] In this study, receptor proteins were produced in forms of cell-derived nanovesicles, purified proteins and synthetic peptides. Their biological signals were monitored by The CNT-based transducers and applied to environmental monitoring, disease diagnosis and food quality assessment.

For the deorphanization of olfactory receptors, artificial olfactory cells were constructed using heterologous reporter gene systems.[8] Specific receptors were screened for detection of potential biomarkers and evaluation of cell surface expression was performed. The cell-derived nanovesicles were constructed for the scalable signal transduction to the CNTs.[9] A CNT-based field-effect transistor (FET) was fabricated via the conventional photolithography process.[10] CNT channels were functionalized with nanovecsicles and the electrical properties of the CNT-FET were also maintained after the immobilization of nanovesicles. The nanovesicle-based bioelectronic sensor detected target biomarkers with high sensitivity and selectivity. The bioelectronic sensor using receptors presented simple rapid analytical methods for water quality monitoring and diabetes diagnosis.

Developing a multiplexed platform and miniaturizing sensing device is necessary for practical applications of bioelectronic sensors. Four kinds of receptor proteins were expressed in *Escherichia coli*, purified and refolded with the detergent micelle methods. The proteins were immobilized onto the multi-type CNT channels which designed for simultaneous detection of the target molecules. A current monitoring device was customized for the multi-

channel CNT-FET and operated by a laptop computer. Complex pattern recognitions of various molecules were available without any interference from non-target molecules. The simple portable bioelectronic device was suitable for efficient assessment of food quality and is expected to be used as a rapid on-site sensing platform.

Receptor protein-derived peptides were synthesized based on the sequence of ligand binding sites and applied to the development of the bioelectronic sensor. The peptides do not require cell membrane-like environments so that they were easily stored.[11] Furthermore, The synthesized peptides could directly immobilized onto the CNTs using the pi-pi interaction by simple modifications with additional phenylalanine residues.[12, 13] The peptide-based bioelectronic sensor detected a serum biomarker of nerumyelitis optica with high specificity. Furthermore, the sensitivity was much higher so that the early-phase detection was available.

In this research, bioelectronic sensor using carbon nanotubes and various types of receptors such as nanovesicles, proteins and peptides were developed for simple and rapid detection of the biomarkers. The developed sensors applied for the environmental monitoring, disease diagnosis and food quality assessment.

Keywords: bioelectronic sensor, receptor, carbon nanotube, environmental monitoring, disease diagnosis, food quality assessment

Student number: 2012-30968

Contents

List of Figures

List of Table

List of Abbreviations

AFM: atomic force microscopy

AQP4: aquaporin-4

BioFET: biologically sensitive field-effect transistor

cAMP: cyclic adenosine monophosphate

CNS: central nerve system

CNT: carbon nanotube

DMEM: Dulbecco's modified Eagle's medium

PBS: phosphate-buffered saline

E. coli: *Escherichia coli*

FBS: fetal bovine serum

FET: field-effect transistor

GC/MS: gas chromatography-mass spectroscopy

GPCR: G protein-coupled receptor

HEK-293: human embryonic kidney-293

NMO: euromyelitis optica

OR: olfactory receptor

ORP: olfactory receptor-derived peptide

OSN: olfactory sensory neuron

OTS: octadecyltrichlorosilane

PCR: polymerase chain reaction

PDL: poly-D-lysine

RTP1S: receptor-transporting protein 1S

SEM: scanning electron microscope

SD: standard deviation

SPME : solid phase micro extraction

TMA: trimethylamine

VOC: volatile organic compound

Chapter 1.

Research background and objective

Chapter 1. Research background and objective

Bioelectronic sensors that integrate biology and electronics have been developed via multidisciplinary approaches. Biological systems in living organisms are operated by internal and external stimuli such as sensory inputs and environmental influences. Receptor proteins are used as primary recognition elements in signal transduction pathways, which trigger activation mechanisms by various stimulations. G protein-coupled receptors (GPCRs) are involved in various processes such as vision, olfaction, taste, nerve functions, metabolism and immune response.[14] Receptor-ligand interactions modulate structural changes of the receptors and cellular responses such as ion influx. These changes can be utilized to develop biosensor using GPCRs.[15] Traditionally, cell-based assays have been used for studying of receptor functions.[16] Since most of the receptor proteins exist in cellular membranes, they requires *in vivo*-like environments for maintaining their functions.

Nanomaterial-based biosensors have been emerged as a promising platform of bio-signal amplifications.[17,18] The use of carbon nanomaterials, such as carbon nanotubes and graphene, has provided the significant advances in biomolecule sensing.[19] Nanomaterial-based FET biosensors have strength in the size comparability and the bio-compatibility.[20] The unique properties of nanomaterials enable the highly sensitive detection of biomolecule and could be applied to receptor protein researches.

Bioelectronic sensors using receptor proteins and carbon nanotubes detected target molecules at single-atom resolution[21], and have potential for various applications: food assessment, quality control, environmental and industrial monitoring, safety controls and medical diagnosis.[22] Human olfactory receptors (hORs)[23,24], taste receptors (TRs)[25] and hormone receptors[26] utilized for mimicking human sensory responses. The

integration of the human-derived receptors into bioelectronic sensor showed higher sensitivity than the previous sensors.

Despite remarkable advances in bioelectronic sensor, bioelectronic sensors are still applied to limited areas. For the practical applications of receptor-based bioelectronic sensors, deorphanization of receptor proteins, proper functionalization strategies of nanomaterials, and multiplexing and miniaturization of sensing platform is required.

In this research, artificial olfactory cells were used for screening of hORs which detect water contamination indicators and diabetes biomarkers. Olfactory nanovesicles containing the selected hORs were immobilized onto a CNT-FET. The nanovesicle-based bioelectronic sensor detected target odorants with high sensitivity and selectivity. Various kinds of ORs and TRs were produced in *E. coli*, and the reconstituted receptors were immobilized onto a multi-channel CNT-FET. A portable current monitoring system was customized with the bioelectronic sensor. Various pattern recognitions were successfully performed with complex mixtures. The protein-based multiplexed bioelectronic sensor was suitable for efficient assessment of food freshness. Simple and stable peptide-based bioelectronic sensors was applied to disease diagnosis and food quality assessment.

In summary, the objectives of this study are:

1. Development of bioelectronic sensor using human olfactory nanovesicles for water quality assessment and diabetes diagnosis
2. Development of portable and multiplexed bioelectronic sensor using human OR and TR proteins for assessment of food quality
3. Development peptide-based bioelectronic sensor using ligand binding sites of receptors for neuromyelitis optica diagnosis and seafood quality assessment

4. Comparison of bioelectronic sensor performances with traditional analytical methods.

In the thesis, the bioelectronic sensors using receptor proteins and CNT were developed. Receptor proteins were produced as nanovesicles, proteins and peptides, and integrated with CNT-FETs. The developed sensors were applied to environmental monitoring, disease diagnosis and food quality monitoring.

Chapter 2.

Literature review

Chapter 2. Literature review

2.1 Concept of bioelectronic sensor

Technical convergence of biotechnology and nanotechnology enable remarkable scientific advances. Various biomolecules such as DNA, protein and cells were integrated with biocompatible nanomaterials.[27] These approaches drive a deeper understanding of biological systems and developing novel analytical tools. Bioelectronic sensor use various kinds of biomolecules as primary recognition elements. Biomolecules have excellent specificity with their target molecules so that they overcome the limitations of chemical sensors.[28] Electronics with carbon nanomaterials such as one-dimensional carbon nanotubes and two-dimensional graphene layers, offer fast response, small, simple, and cheap transistor.[29] Owing to the excellent properties of carbon nanomaterials, nanomaterial-based biosensors have been extensively developed.[30,31] Especially, biologically sensitive field-effect transistors (BioFETs) that measure biological action potentials and change conductivity of source-drain, have been have emerged as an extremely sensitive and selective sensing platforms.[32,33] Following steps are required for the development of bioelectronic sensor; 1) production of suitable biomolecules for the ligand detection,[34] 2) stable immobilization of biomolecules onto an electronic sensor surface,[35,36] 3) conversion of biological signals into electrical signals.

2.2 Biomolecules as primary recognition elements

2.2.1 DNA

DNA is a molecule that contains the genetic information of living organisms in genome sequences.[37] Human genome project provide us entire DNA sequences and thus helps understanding gene-disease relationships.[38] Since DNA molecules are negatively charged, their interactions can be detected using the BioFET platform.[39] The hybridization of a complementary DNA onto the DNA-modified FET sensor influences the charge density distribution of the sensor surface.[40] DNA-based sensors can be applied to the sequencing [41]and the identification of single nucleotide polymorphisms.[42] DNA and aptamer are also utilized as primary recognition elements of the BioFET sensor for the detection of chemical warfare agents[43] and enzymes.[44]

2.2.2 Protein

Protein is a macromolecule that performs various functions in catalytic reactions and signal transductions. Protein 3D structures have the specific ligand binding sites so that the proteinsca be used as selective recognition elements of biosensors. Enzymes, antibodies and receptors are most frequently used for the development of biosensors.[45] Enzyme-substrate reactions were applied to the glucose sensing using glucose oxidase for the diagnosis and management of diabetes.[46] Oxygen, an additional product of the glucose oxidation reaction, have the reduction potentials to the FET sensor surface.[47] Antibody-antigen interactions were applied to the cancer diagnosis for the detection of prostate-specific antigen (PSA).[48] The specific binding activity of antibodies have great potentials for the development of novel diagnostic tools. Recently, receptor proteins that exist on the cell

membrane have been utilized for the development of BioFETs.[49,50] Since receptor proteins require complex environmental conditions such as cell membrane structures, examples are relatively small.[51] Crucial roles of receptor proteins in biological systems are applied to disease diagnosis, drug discovery and sensory stimulations. Furthermore, reprograming of receptor protein activity is available based on an *in silico* modeling of protein structures.[52] Changes of the specific protein sequence are related to the selectivity of proteins. More diverse applications are expected with the delicate engineering of the receptor proteins.

2.2.3 Cell

Cell is a basic unit of organisms that is composed of many biomolecules such as proteins and nucleic acids. Cells can be grown on biocompatible nanomaterials and their activities can be measured by the BioFETs.[53] Carbon nanotubes, graphene and silicon nanowires have been reported as nanomaterials for cell culture matrices.[54] Cell-based BioFETs provide high-resolution observations of cellular signals, and detailed understanding of the biological system such as cell biology, toxicology and pharmacology. For examples, neuronal exon signals were monitoring using the silicon nanowire array[55] and neuron transmitter was detected using the carbon nanotube transistor.[56] However, cell-based sensors have limitations in their applications such as reliability, reusability and stability. Recently, monitoring of non-adherent cell activities using floating-electrode also reported as a reusable platform.[57] Toward more scalable integration of cell components, cell-derived nanovesicles was also utilized for the developmend of the BioFETs.[24]

2.3 Nanomaterials as secondary signal transducers

2.3.1 Carbon nanotube

CNTs are one-dimensional nanomaterials that made from one layers of graphite. CNTs have unique structural, electronic and chemical properties that are useful for biosensing applications.[58] CNTs are divided into two types: single-walled nanotubes (SWCNTs) made of a single carbon layer, and multi-walled nanotubes (MWCNTs) made of several nested tubes. Large-scale fabrication techniques for CNTs are developed using linker-free directed assembly, and it is expected to lead to the mass production of bioselectronic sensors.[59] The surface of CNTs can be covalently modified using pi-interactions,[60] and non-covalently modified using hydrophobic interactions.[61] These strategies offer opportunities for the immobilization of various biomolecules. CNTs have p-type FET characteristics and current changes in the sensing channels are sensitively measured (Figure 2.1).

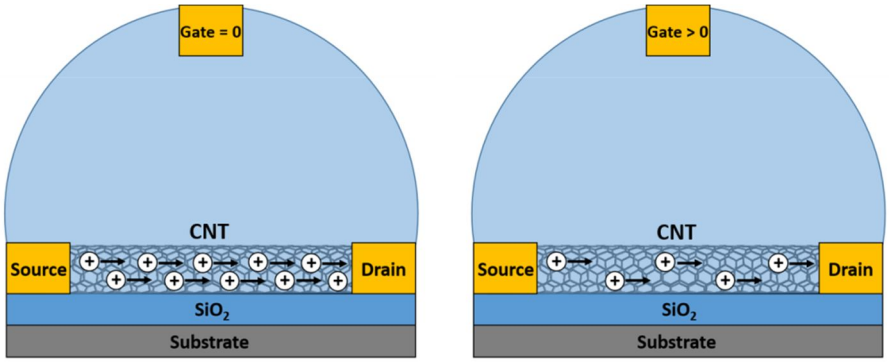

Figure 2.1 A sensing principle of CTN-FET. CNT-FETs have p-type properties and hole charge carriers are dominant in the current flow. The number of holes decreases with a positive gate voltage and the current signal decreases.

2.3.2 Conducting polymer

Conducting polymers are organic polymers that have the electrical conductivity, and their properties for biosensing applications can be controlled by a doping/dedoping process.[62] Large surface area and porous structures of conducting polymers are regarded as advantages for rapid biosensing platforms.[63] Polyaniline (PANI), polypyrrole (PPy), polyacetylene (PAc), polyphenylene(PPP) and polythiophene (PT) are commonly used for the development of the biosensors.[64] Physical adsorption,[65] entrapment,[66] cross-linking[67] and covalent bonding[68] have been used for the biomolecule immobilization onto conducting polymers. Furthermore, conducting polymer hydrogels (CPHs) that combine hydrogels and organic conductors, provide high water contents and 3D nanostructures, which are required for the development of the biosensor.[69,70]

2.3.3 Graphene

Graphene is a two-dimensional material form of carbon that have unique physicochemical properties for such as high surface area, excellent conductivity, high mechanical strength, and ease of functionalization.[71] Graphene can be easily produced by the peeling-off methods[72] and chemical vapor deposition (CVD) methods can produce large areas of a single layer graphene.[73] Graphene-based biosensor was sufficiently biocompatible to be used for *in vitro* and *in vivo* monitoring.[74] Furthermore, the hybrid structures of polymers and graphene improve the performances and expand their applications.[75] The ability to modulate the properties of graphene-based sensor means that is able to develop a sensor that can operate in desired conditions. Flexible graphene-based capacitors have been developed with the laser scribing method.[76] It is expected to develop wearable devices using flexible arrays of bioelectronics on human skin.

2.4 Bioelectronic sensors using receptor proteins

2.4.1 Bioelectronic nose

Bioelectronic noses that use human olfactory receptors as primary recognition elements and nanomaterials as secondary transducers have been reported.[77] In the human nose, odor molecules binds to olfactory receptors in olfactory sensory neurons of the olfactory epithelium.[78,79] The activated neurons deliver electrical signals to the glomerulus and the signals are transmitted to the higher regions of the brain.[80] Humans have approximately 400 functional olfactory receptors and combinatorial odor binding patterns of the receptors could discriminate more than 10,000 different odors.[81,82,83] In the bioelectronic nose platform, human olfactory receptors selectively distinguish target ligands with a single atomic resolution like human nose do,[84] and their electric potential changes are converted into a field effect of the transistor sensor.[85] The transistor circuit based on the nanomaterials, such as carbon nanotubes,[86] graphene[87] and conducting polymers,[88] rapidly and sensitively amplify the biological signals. Advantages of the specific odor binding of the olfactory receptor and rapid signal transduction of nanomaterials have been used in various applications. Bioelectronic noses detect potential biomarkers such as heptanal (a serum biomarker of lung cancer) for disease diagnosis,[89] geosmin and 2-methylisoborneol (water contamination indicatiors) for environmental and industrial monitoring,[90] hexanal (a lipid oxidation indicator),[91] trimethylamine (a seafood decomposition indicator)[92,93] and 1-octen-3-ol (a fungal contamination indicator of grain)[94] for food quality assessment. Bioelectronic nose rapidly detects target molecules with simple manipulations compared with the conventional methods that require complex pretreatment and large instruments. The miniaturized platforms with the bioelectronics enable

portable sensing systems for on-site analysis of odor compounds. Furthermore, the human olfactory receptor-based bioelectronic nose that mimics the human smell sensing mechanism indicates the complex pattern recognition of the olfactory system with the multiplexed platform.[95] The multiplexed bioelectronic nose is composed of various human olfactory receptors in the sensor array networks and quantify the response of stimulated olfactory receptor signals. The sensor array networks combine olfactory signals like olfactory sensory neurons do in the human nose[96] and computer process define the olfactory code like the human brain.

2.4.2 Bioelectronic tongue

Bioelectronic tongue that combines human taste receptors and -electronics, mimics the human taste systems and their various applications have been reported.[50] Humans are known to have the five basic tastes; sweet, sour. Bitter, salty and umami.[97] In the human tongue, tastants are recognized by different cells expressing specific taste receptors. There are two opinions for the taste quality coding; labelled-line model[98] and across-fibre models.[99] GPCRs for umami, sweet and bitter are previously identified; umami: T1R1+T1R3 heterodimer,[100] sweet: T1R2+T1R3 heterodimer,[101] and bitter: about 30 T2Rs.[102,103] These receptors are utilized for the development of biolectronic nose and their human-like performances were evaluated. CNT-FET using human bitter receptor protein,[104] CNT-FET using human sweet receptor nanovesicle,[25] CPNT-FET using human bitter taste receptor protein,[105] and CNT-FET using insect umami nanovesicle[106] have been reported.

2.4.3 Applications

Various applications of bioeletronic sensors using receptors have been reported (Table 2.1). A chemical-pain sensor is constructed with rat pain sensory receptor rTRPV1 and nanovesicle-based CNT-FET.[107] The chemical-pain sensor detects capsaicin with a high sensitivity and expected to be utilized for drug screening systems. A disease specific antibody sensor is constructed with aquaporin-4 and nanovesicle-based CNT-FET.[108] The antibody sensor detects AQP-IgG and related biomedical applications such as disease diagnostics. A dopamine biosensor is constructed with human dopamine receptor nanovesicles and conducting polymer nanomaterials.[109] The dopamine sensor can be applied to the diagnosis of Parkinson's disease. A hormone biosensor is constructed with human parathyroid hormone receptor and carboxylated polypyrrole nanoparticles.[110] The peptide hormone sensor can be applied to analyze hormone imbalance in human body. For the development of applicable sensors in various fields, the produced receptor proteins should be functional and stable. In addition, the proper immobilization steps onto nanomaterials are required according to different types of protein.

Table 1. Applications of bioelectronic sensors using receptor proteins

Primary recognition	Secondary transducer	Receptor	Ligand	Application	Reference
Nanovesicle	CNT	hOR1J2	Heptanal	Lung cancer diagnosis	89
	CNT	cfOR5269	Hexanal	Lipid oxidation in dairy products	92
	CNT	hOR8H2	1-octen-3-ol	Fungal contamination in grain	94
	CNT	hTAS1R2, hTAS1R3	Sucrose	Sweet taste analysis	25
	CNT	AmGr10	MSG	Umami taste analysis	106
	CNT	rTRPV1	Capsaicin	Chemical pain analysis	107
	CNT	Aquaporin 4	AQP4-IgG	NMO diagnosis	108
	CPEDOT	hDRD1	Dopamine	Parkinson disease diagnosis	109
Protein	CNT	hTAS2R38	PTC, PROP	Bitter taste analysis	105
	CNT	M1 mAChR	Acetylcholine	Neurotransmitter analysis	26
Peptide	CPPyNPs	hPTHR	hPTHR	Hormone imbalance analysis	110
	CNT	hORP61m	TMA	Seafood decomposition	92, 93

Chapter 3.

Experimental procedures

Chapter 3. Experimental procedures

3.1 Gene cloning

All receptor genes were amplified by polymerase chain reaction from human genomic libraries. Human ORs were cloned with sequence information from the Olfactory Receptor DataBase. All hORs were subcloned in pcDNA3 mammalian expression vectors (Invitrogen, USA) containing the first 20 amino acids of human rhodopsin (Rho-tag) (Zhuang and Matsunami, 2007). Human OR2J2, 2W1, TAAR5, and TAS2R38 were cloned in the pET-DEST42 *E. coli* expression vector (Invitrogen, USA) containing a 6xHis-tag. The sequences of the cloned genes were verified by sequencing (GenoTech, Korea).

3.2 Production of receptor proteins

3.2.1 Mammalian expression

Human embryonic kidney (HEK)-293 cells were cultured in Dulbecco's Modified Eagles Medium (DMEM) (HyClone, USA) supplemented with 10% Fetal Bovine Serum (FBS) (Gibco, USA) and 100 U/ml penicillin, 100 μg/ml streptomycin (Gibco, USA) at 37°C and 5% CO_2. Transfection was performed with the Neon Transfection System (Invitrogen, USA). The cells were harvested and resuspended in phosphate-buffered saline (PBS) and 2 x 10^6 cells were mixed with 5 μg of OR, 2 μg of pCRE-Luc, 1 μg of pSV40-RL, 1 μg of RTP1S, 0.5 μg of Ric8b, 0.5 μg of $G_{\alpha olf}$. Electric pulses were then applied three times at 1100 V with 10 ms per pulse. Transfected cells were cultured in DMEM supplemented with 10% FBS without antibiotics, with 5 x 10^4 cells per well in 96-well plates.

3.2.2 Bacterial expression

The BL21(DE3) *E. coli* was transformed and incubated in LB medium containing 100 μg/ml ampicillin at 37°C. The expression of the receptor proteins was induced at 0.5 OD_{600} with 0.5 mM IPTG, and incubated for 4 h. The cells were harvested by centrifugation (4°C, 7,000 g, 30 min) and resuspended in PBS containing protease inhibitors. The resuspended cells were lysed by sonication with 5 s on/off for 10 min (Sonics Vibracell, USA), and the lysates were solubilized in 0.1 M Tris-HCl (pH 8.0), 20 mM SDS, 1 mM EDTA, and 100 mM DTT at room temperature. The solubilized proteins were dialyzed in 0.1 M sodium phosphate and 10 mM SDS buffer (pH 8.0) with a 10K MWCO membrane (Thermo Scientific, USA), and filtered through a 0.2 μm syringe filter (Pall Life Sciences, USA). The proteins were then purified by a His6 Ni gravity column (Clonetech Laboratories, USA), and equilibrated with 0.1 M sodium phosphate and 10 mM SDS (pH 8.0), washed with 0.1 M sodium phosphate and 10 mM SDS (pH 8.0 and then pH 7.0), and eluted from the column with pH 6.0. The eluted proteins were dialyzed in 0.1 M Tris-HCl, 10 mM SDS, 0.5 mM EDTA (pH 8.0) and 0.1 M Tris-HCl, 3 mM SDS, 0.5 mM EDTA (pH 8.0). For the reconstitution of receptors, 1 mM GSSG, 6 mM GSH, 6 mM DDM, 6 mM Cymal 6, and 6 mM MβCD were added, and the solution was stored at -20°C for 48 h. The samples were thawed at 4 °C and 25 mM $CaCl_2$ was added. Finally, the samples were dialyzed in 100 mM Tris-HCl, 300 mM NaCl, 10% glycerol, 1 mM DDM, 1 mM Cymal 6, and 1 mM EDTA (pH 7.4). The secondary structure of the reconstituted protein samples was analyzed using a CD spectrometer (Applied Photophysics, UK) at wavelengths between 200 and 250 nm. Their functionality was analyzed by a tryptophan fluorescence quenching method using a luminescence spectrometer (Perkin Elmer, USA) (excitation 290 nm, emission 350 nm).

3.2.3 Construction of nanovesicles

HEK-293 cells were resuspended in serum-free DMEM containing 10 μg/ml of cytochalasin B (Sigma, USA) and agitated at 300 rpm for 30 min. The nanovesicles were separated from the cells by centrifugation at 500 g for 10 min, and the supernatant was centrifugated to collect the nanovesicles at 15000 g for 30 min. The produced nanovesicles were resuspended in PBS with 1 μg/ml of total protein concentration, stored at -70°C, and melted before being use.

3.2.4 Synthesis of peptides

Human olfactory receptor-derived peptide (horp61m: NQLSNLSFSDLFFF) and three kinds of AQP4 extracellular loop peptides (A : GGSENPLPVFFF, C : TPPSVVGGLGVTTVHGNLTAGFFF, E : GNWENHWFFF) with purity higher than 95% were purchased from Peptron (Korea). All peptides were dissolved and diluted at 1 mg/ml with distilled water. The diluted peptide solution was stored at -20°C and thawed before used.

3.3 Characterization of receptor proteins

3.3.1 CRE-Luciferase reporter gene assay

The Dual-Glo Luciferase Assay System (Promega, USA) was used to measure receptor response. Approximately 24 hours after transfection, the medium was replaced with 50 μl of DMEM and incubated for 30 min at 37°C. After stimulation with 25 μl of odorants for 4 hours at 37°C, luminescence was measured with Luminoskan Ascent Microplate

Luminometer (Thermo Scientific, USA). The luciferase activity was normalized with the formula [CRE/Renilla(N) – CRE/Renilla(0)]/[CRE/Renilla(FSK) – CRE/Renilla(0)]. 1 μM forskolin (FSK), an adenylyl cyclase activator, was used as a positive control and a no-odorant solution was used as a negative control for each hOR.

3.3.2 Calcium influx assay

HEK-293 cells were incubated for 30 min with 10 μM of Fura-2 AM (Invitrogen, USA) in Ringer's solution (140 mM NaCl, 1 mM $MgCl_2$, 1.8 mM $CaCl_2$, 5 mM KCl, 5 mM glucose, 10 mM HEPES (pH 7.4)) at 37°C. The Fura-2 AM-loaded nanovesicles were produced as described for the formation of regular nanovesicles and placed on a 96-well plate. Calcium-dependent fluorescence was measured at 510 nm with dual excitations at 340 nm and 380 nm using a GENios Pro microplate reader (TECAN, Switzerland).

3.3.3 Immunocytochemistry

HEK-293 cells were fixed with 4% paraformaldehyde in PBS at room temperature for 20 min. The cells were blocked with 5% BSA diluted in PBS and incubated with the Rho-tag antibody at a 1:500 dilution in PBS with 5% BSA at 37°C for 1hour. The cells were then washed three times with PBS and incubated with the Alexa Fluor 594 (Invitrogen, USA) at 1:1000 dilution in PBS with 5% BSA at 37°C for 1hour.

3.3.4 Western blot analysis

HEK-293 cells and nanovesicles were washed twice with PBS and lysed by sonication (2s on/off, 5 min). The supernatant and membrane fractions

were separated by centrifugation at 15000 g for 30 min. Protein samples were loaded onto 10% SDS-PAGE gels and transferred to PVDF membranes (Bio-Rad, USA) under 0.15 A of constant current for 60 min. The membranes were blocked with 5% BSA diluted in PBS and 0.1% Tween-20 at room temperature for 1 hour and incubated overnight with the Rho-tag antibody at a 1:1000 dilution in PBS with 5% BSA and 0.1% Tween-20 at 4°C. The membranes were then washed three times for 5 min with PBS with 5% BSA and 0.1% Tween-20 and incubated with anti-rabbit IgG-HRP (Invitrogen, USA) at 1:1000 dilution in PBS with 5% BSA and 0.1% Tween-20 at room temperature for 1 hour. ECL solution (Thermo Scientific, USA) was used to detect proteins expressed on the membrane.

3.3.5 Scanning electron microscopy

HEK-293 cell-derived nanovesicles were applied on poly-D-lysine-coated slide glass and fixed with 4% paraformaldehyde in PBS at room temperature for 20 min. The fixed nanovesicles were dehydrated with increasing concentrations of ethanol and lyophilized by freeze-drying. The lyophilized nanovesicles were coated with Pt (10nm) by a sputtering method and visualized by SEM.

3.4 Construction of in vitro disease models

3.4.1 Cultivation of adipocytes and skeletal muscle cells

Pre-adipocytes 3T3-L1 were maintained in DMEM (Hyclone, USA) supplemented with 10% calf serum (Gibco, USA), and differentiated into adipocytes with a DMI medium (DMEM, 10% FBS (Gibco, USA), 500 μM IBMX, 5 μg/ml insulin, 250 nM dexamethasone). The differentiation medium was removed after 2 days and replaced with DMEM supplemented

with 10% FBS and 1 μg/ml insulin. The medium was replaced every 2 days with DMEM supplemented with 10% FBS, 10-12 days post differentiation. Myoblasts L6 were maintained in DMEM supplemented with 10% FBS, and differentiated into skeletal muscle cells with DMEM containing 2% horse serum, 5-7 days post differentiation.

3.4.2 2-Deoxyglucose uptake assay

Glucose Uptake Cell-Based Assay Kit (Cayman Chemical, USA) was used to analyze the glucose uptake activity of the cells. The differentiated cells were serum-starved for 12 hours in DMEM containing 0.2% BSA. The cells were cultured for 24 hours in DMEM containing 0.5 mM palmitic acid. After washing two times with PBS, the cells were incubated with KRB ringer's solution containing 100 nM insulin for 30 min (adipocytes) and 60 min (skeletal muscle cells) at 37°C. Then, the cells were incubated with KRB ringer's solution containing 150 μg/ml 2-NBDG for 10 min at at 37°C. The incubated cells were washed two times with PBS and fluorescence was measured at 535 nm with excitation at 485 nm using a GENios Pro microplate reader (TECAN, Switzerland).

3.4.3 GC/MS analysis

The volatile organic compounds (VOCs) in the headspace of the cells were analyzed using Trace GC Ultra gas chromatography (Thermo Scientific, USA) with an ITQ1100 mass spectrometer (Thermo Scientific, USA). Before experiments the cell culture medium was replaced with the fresh DMEM, and 65 μm PDMS/DVB-coated SPME fiber (Supelco, USA) was placed on the headspace. The fiber was incubated for 16 hours at 37°C, and injected to the GC/MS. The inlet temperature was 250°C. The column temperature was maintained at 40°C for 4 min and increased to 230°C at the

rate of 5°C/min, and maintained for 4 min. The temperatures of the ion source and the mass transfer line were 260°C and 285°C, respectively. The detected VOCs were identified by the NIST library.

3.5 Fabrication of bioelectronic sensor

3.5.1 Fabrication of CNT-FET

Purified swCNTs (Hanwha, Korea) were dispersed in 1,2-dichlorobenzene solution by applying ultrasonic vibration for 1 hour. To create swCNTs patterns on a silicon oxide wafer, the octadecyltrichlorosilane (OTS) self-assembled monolayer (SAM) technique was used. First, we patterned AZ5214 photoresists on a silicon oxide wafer by using a conventional photolithographic technique. Then the wafer was placed in an OTS solution (1:500, v/v in hexane) for 5 min to create OTS SAM on the wafer. Subsequently, the OTS-coated wafer was dipped in acetone to remove the AZ5214 patterns. Next, the OTS-patterned wafer was placed in the swCNT solution for 30 s. These steps allowed swCNTs to be adsorbed selectively onto bare silicon oxide regions in the wafer, while OTS SAM regions blocked the adsorption of swCNTs. Source and drain electrodes (Au/Pd, 30 nm/10 nm) were fabricated via conventional photolithography, thermal evaporation, and lift-off process. Finally, the source and drain electrodes were passivated with a photoresist to prevent current leakage from the electrodes.

3.5.2 Fabrication of multi-channel CNT-FET

A silicon oxide substrate was patterned for swCNT assembly. The patterned SiO_2 (300nm) wafer was placed in the OTS solution (OTS: Hexane = 1 : 400) for 7 min to form a self-assembled monolayer of OTS, so

that the OTS patterned regions were non-polar. The OTS patterned wafer was placed in the swCNT (Sigma Aldrich, USA) solution (0.02mg/ml in 1,2-dichlotobenzene) for 30 s and rinsed thoroughly with 1,2-dichlotobenzene. swCNT was selectively absorbed on the empty SiO_2 regions due to the self-assembled OTS layer. Subsequently, the Ti/Au (100/300 nm) electrodes were developed via a thermal evaporation method. Finally, the passivation layers were fabricated on the electrode regions to prevent leakage currents of during the experiments under aquatic conditions. swCNTs of the MCS (multi-channel sensor) were functionalized with nickel ions following a previously reported method. The MCS was placed in 10 mM 4-carboxybenzene diazonium tetrafluoroborate solution at 45 ℃ for 1 h, followed by washing with acetone, methanol, and water. An activation buffer was prepared with 0.1 M 2-(N-morpholino)ethanesulfonic acid sodium salt (MES) and 0.5 M NaCl (pH 6.0 adjusted with HCl). The MCS was placed in 2 mM EDC and 5 mM Sulfo-NHS in the activation buffer at room temperature for 15 min, in order to activate the carboxylic acid of 4-carboxybenzene diazonium tetrafluoroborate. The MCS was then washed with activation buffer and placed in 11.3 mM NTA-NH_2 in PBS solution for 2 h. Subsequently, the MCS was washed with DI water and placed in 11.3 mM $NiCl_2$ for 1 h. Upon completion, the MCS was thoroughly washed with DI water and dried with N_2.

3.5.3 Immobilization of nanovesicle

For the immobilization of nanovesicsles, 0.1 mg/ml of poly-D-lysine in PBS was added to CNT channel regions and incubated at room temperature for 2 hours. Then, 1 μl of nanovesicles in PBS was added to the swCNT channel and the mixture was incubated at 4°C for 2 h. Nanovisicles containing receptor proteins immobilized onto CNT channel using charge-charge interactions.

3.5.4 Immobilization of protein

For the direct immobilization of His-fused receptor proteins onto Ni-decorated CNT channels, 1 μM reconstituted protein was placed on each channels for 30 min at 4°C. Receptor proteins were immobilized onto CNT channels using His-Ni interactions.

3.5.4 Immobilization of peptide

For the immobilization the receptor-derived peptides, 1 μg/μl of peptide solution was placed on the CNT channel of the fabricated CNT-FET for 4 h. After immobilization, unbound peptides were washed 3 times with distilled water. Phe-modified Peptides were immobilized CNT channels using pi-pi interactions.

3.5.5 Characterization of nanovesicle immobilization using SEM

Nanovesicles on CNT channels were fixed with 4% paraformaldehyde in PBS at room temperature for 20 min. The fixed nanovesicles were dehydrated with increasing concentrations of ethanol and lyophilized by freeze-drying. The lyophilized nanovesicles were coated with Pt (10nm) by a sputtering method and visualized by SEM.

3.5.6 Characterization of receptor and peptide immobilization using AFM

The imaging of CNT channels were performed using AFM (Asylum Research, USA) under ambient conditions. At first, the

pristine CNT channels were imaged in tapping mode with a scan rate of 0.2 Hz. After the immobilization of the proteins and peptides, AFM imaging of the CNT channels was performed in the same mode at 0.1 Hz to avoid undesired noise.

3.6 Electrical measurement

3.6.1 Single-channel CNT-FET

For the electrical signal measurement, 20 µl of PBS with pH 7.4 was added to the CNT channel. A 0.1 V bias voltage was applied between the source-drain electrodes, while the gate voltage was grounded. Current changes were monitored with a 2636A Dual-channel system source meter instrument (Keithley, USA) and a MST 8000 probestation (MS TECH, Korea).

3.6.2 Multi-channel CNT-FET

For the simultaneous detection of four individual channels for one set, 49.5 µl PBS buffer was placed on the multi-type CNT channels and 0.5 µl standard molecules or food samples were injected into the sensor. After 30 s, the current signals of each channel were monitored using the HyperTerminal software. All standard molecules were serially diluted 1:10 using PBS and stored at 4°C until used. All foods; banana (Philippines), beef sirloin (Australia), broccoli (Korea), cabbage (Korea), sliced cheese (Korea), chicken breast (Korea), milk (Korea), oyster (Korea), pork sirloin (Korea), potato (Korea), white leg shrimp (Iran), and strawberry (Korea) were purchased from a local market and stored at 4°C. For the preparation of food samples, 1 ml PBS buffer was added to 1 mg food, and their liquid fractions were diluted 1:100 before use in the experiments.

Chapter 4.

Development of bioelectronic sensor using human olfactory nanovesicles for the detection of odor compounds in water pollution

Chapter 4. Development of bioelectronic sensor using human olfactory nanovesicles for the detection of odor compounds in water pollution

4.1 Introduction

Water is one of the most important resources for biological systems, not only for human being but also for all known living organisms. With growing interest in environmental pollution, water contamination has emerged as an important issue. When water is contaminated by bacteria, various off-flavors are produced such as geosmin (GSM) and 2-methylisoborneol (MIB), which release an earthy and musty odor, respectively.[111,112,113] A human nose is extremely sensitive to these molecules[114] and these compounds are regulated by law for safe drinking water. In addition, harmful algal bloom, which occurs with high bacterial densities and increased water temperature, can be recognized by the smells of GSM and MIB.[115]

Typically, solid-phase microextraction gas chromatography-mass spectrometry (SPME-GC/MS) is used for the detection of GSM and MIB in water supply system.[116,117] Although conventional methods have the advantage of a quantitative component analysis, they have limitations in rapid on-site assessments of water quality due to their long and complex pretreatment procedures, and large-sized instrumentations. Additionally, the equipment is too complicated for beginners, and requires expert operators.

Recently, the bioelectronic nose, which integrates of olfactory receptors (ORs) found in natural system and nanomaterials such as carbon nanotube,[24,84,86,89,91,92,118] conducting polymer[88] and graphene[87], has been reported as an effective analytical tool for detecting various volatile organic compounds with high selectivity and sensitivity[22,77].

Herein, we report a human olfactory receptor (hOR)-based bioelectronic nose that mimics the human smell sensing mechanism for the fast and easy assessment of water quality by detecting GSM and MIB. The bioelectronic nose is composed of single-walled carbon nanotube (swCNT) field-effect transistor (FET) functionalized with hOR expressing cell-derived nanovesicles. We demonstrate that this bioelectronic nose can serve as a sensor to monitor water quality in real time and even on the spot by directly detecting water contaminants without complex pretreatment processes.

4.2 Screening of human olfactory receptors

In human olfactory senses, numerous smells are recognized by the binding pattern of the odorants with hORs in olfactory sensory neurons.[81,119] The majority of the hOR to ligand binding patterns are unknown and extensive efforts to deorphanize the hOR ligands were undertaken using various methods. To identify the specific receptors for the recognition of GSM and MIB, we constructed libraries comprising of 193 different olfactory receptors representing around 50% of the total hORs and cAMP response element (CRE)-luciferase reporter gene assay was performed with human embryonic kidney (HEK)-293 cells expressing 193 kinds of hORs.[8,120] In the primary screening, we stimulated each hOR with 1 mg/l of odorants in triplicate, and the receptors that responded were selected for a secondary screen (Figure 4.1(a)). Then, the specificity of the selected hORs was identified by applying five standard odorants of drinking water: GSM, MIB, 2,4,6-Trichloroanisole (TCA), 2-Isopropyl-3-methoxypyrazine (IPMP) and 2-Isobutyl-3-methoxypyrazine (IBMP). Based on the results, hOR51S1 and hOR3A4 were selected as specific receptors for GSM and MIB, respectively (Figure 4.1(b)). Furthermore, the successful expression of hORs in the cell membrane was confirmed by immunocytochemistry (Figure 4.2(a)) and Western blot analysis (Figure 4.2(b)).

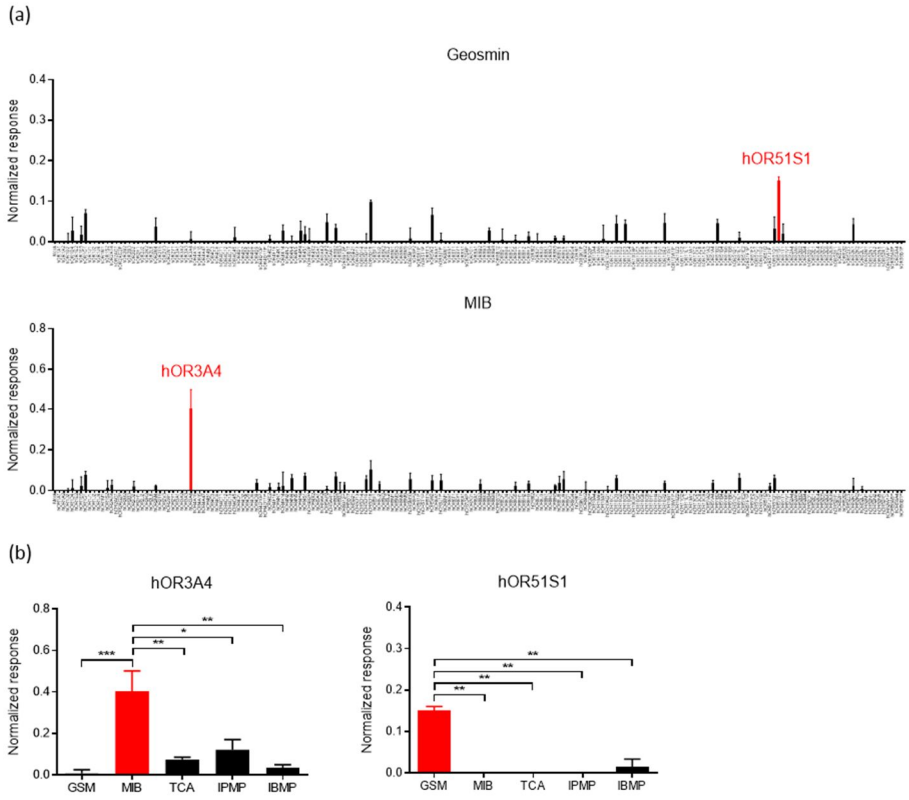

Figure 4.1 Screening of human olfactory receptors. (a) Responses of 193 human olfactory receptors to 1 μg/ml of GSM and MIB. (b) Selectivity of hOR3A4 and hOR51S1. The experiments were performed using 1 μg/ml of 5 drinking water odor standards. Error bars, s. e. m. three replicates. * $P < 0.05$, ** $P < 0.01$, ***$P < 0.001$

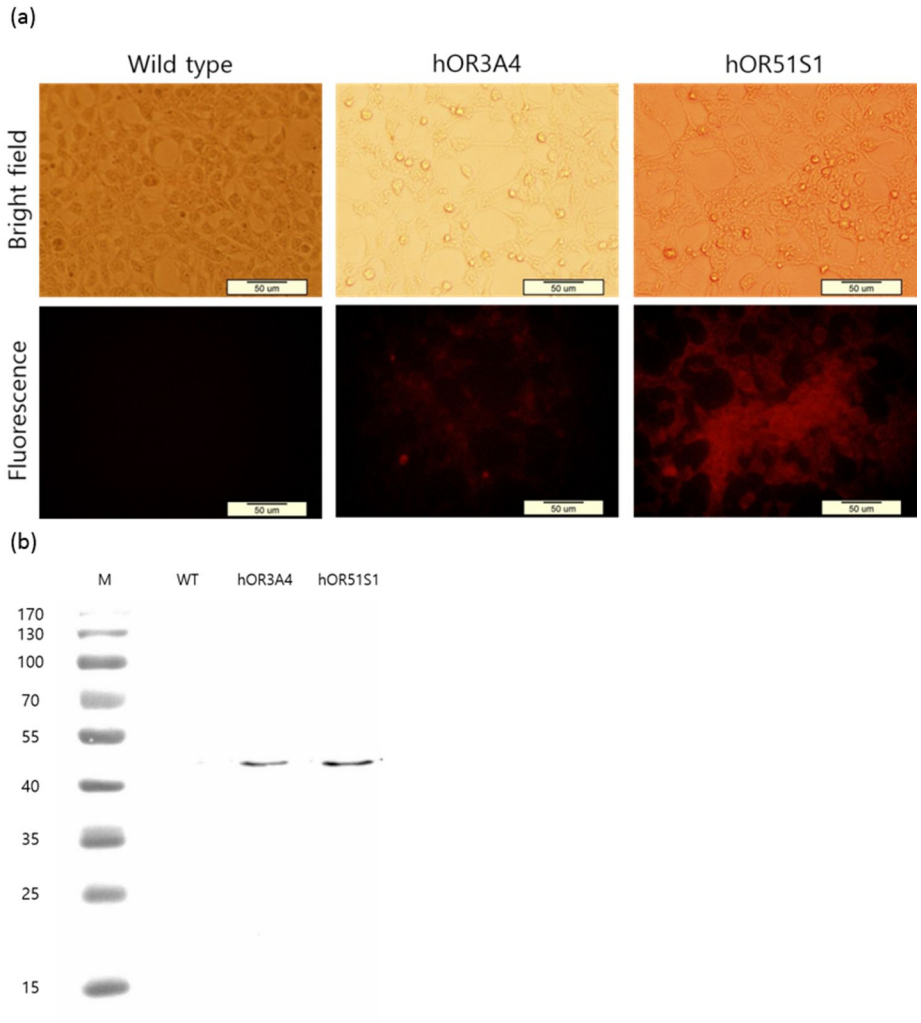

Figure 4.2 Expression of human olfactory receptors in mammalian cells. (a) Immunocytochemistry of hOR3A4 and hOR51S1 expressed in HEK-293 cell surface. (b) Western blot analysis of hOR3A4 and hOR51S1 expressed in HEK-293 cell membrane.

4.3 Characterization of olfactory nanovesicles

Due to their large size and unstability, mammalian cells are not suitable for the functionalization of nanomaterials such as carbon nanotubes. To solve this problem, nanovesicles were produced from HEK-293 cells expressing either hOR3A4 or hOR51S1 by treatment with cytochalasin B, an agent that destabilizes cytoskeleton-membrane interactions.[9] Nanovesicles were released from cytochalasin-treated cells by 300 rpm agitation and collected by sequential centrifugation. The produced olfactory nanovesicles had a sphere-like appearance (Figure 4.3(a)) and their diameters were approximately 100 nm (Figure 4.3(b)). The presence of olfactory receptors in the nanovesicles was confirmed by Western blot analysis (Figure 4.3(c)). Human ORs in the nanovesicles were observed at the expected molecular weight size, whereas no band was observed with control cell-derived nanovesicles. Olfactory receptor activity in the nanovesicles was confirmed by calcium assay with calcium ion-selective fluorescent dye (Figure 4.3(d)). With only hORs in the nanovesicles, the fluorescence signal increased after injection with 100 mg/l of odorants. Furthermore, mass production of the olfactory nanovesicles was possible and they are reported to be stored at -70°C for several weeks without loss of their functional activity.[9] These results indicated that the hORs and their activities were both maintained in nanovesicles and hORs could be used for the functionalization of nanomaterials.

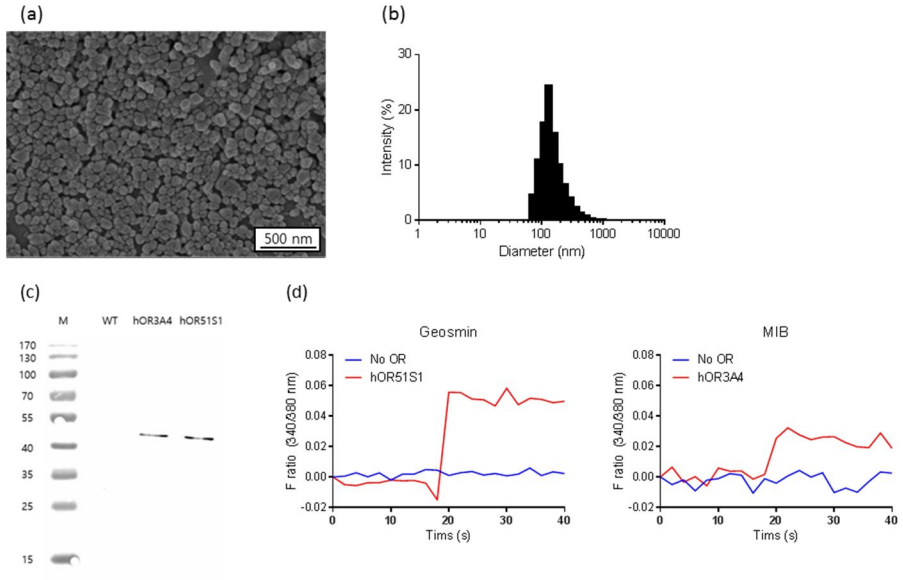

Figure 4.3 Characterization of olfactory nanovesicles (a) SEM image of nanovesicles. (b) Measurement of size distributions via electrophoretic light scattering. (c) Western blot analysis of hOR3A4 and hOR51S1 in nanovesicles. (d) Calcium ion influx assay of nanovesicles with the addition of 1 mg/l of odorants.

4.4 Construction of nanovesicle-based bioelectronic nose

The swCNT surface was treated with positively charged poly-D-lysine (PDL) and functionalized with the olfactory nanovesicles using a charge-charge interaction caused by negatively charged nanovesicle membranes (Figure 4.4(a)). The bioelectronic nose is designed to contain two channels for the simultaneous detection of GSM and MIB. And each channel is functionalized with nanovesicles carrying hOR3A4 and hOR51S1, respectively (Figure 4.4(b)). As a result, the bioelectronic nose can detect GSM and MIB simultaneously. When the bioelectronic nose is exposed to odorants, the binding between ORs and odorants induce a signal transduction with human smell sensing mechanism. This signal transduction results in the influx of Ca^{2+} ion into the nanovesicles and gives a field effect on the swCNT-FET. Successful immobilization of nanovesicles on the swCNT channel was confirmed by SEM image (Figure 4.4(c)). Source-drain current-voltage (I_{SD}-V_{SD}) characteristics for each of the channels were measured to identify the electrical properties of the bioelectronic nose (Figure 4.4 (d)). The observed curves were linear over a voltage range from -0.4 V to +0.4 V, showing the stable ohmic behavior of the swCNTs before and after the functionalization with olfactory nanovesicles in both channels. Although the dI/dV values decreased after the functionalization of the swCNTs due to the increasing resistance, the linearity of the I_{SD}-V_{SD} curve was maintained. We constructed a liquid-ion gated FET system with PBS (pH 7.4) as the electrolyte. The source-drain currents of both channels decreased with an increasing gate voltage before and after immobilization of the olfactory nanovesicles, indicating p-type behavior in both channels (Figure 4.4(e)). These electrical characteristics indicate that the bioelectronic nose can be used as a biosensor for the detection of target molecules.

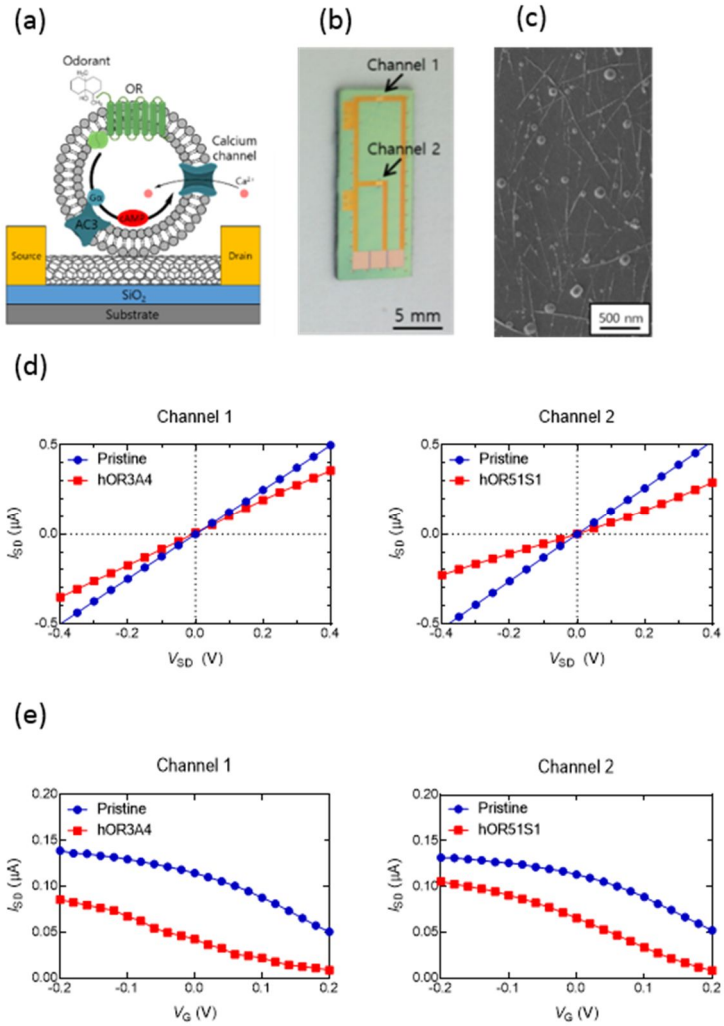

Figure 4.4 Characterization of nanovesicle-based bioelectronic nose. (a) Schematic diagram showing the structure of a bioelectronic nose. (b) Optical image of a bioelectronic nose. CNT channels are indicated by black arrows. (c) SEM images of CNT channels functionalized with olfactory nanovesicles. (d) Current-voltage (I_{SD}-V_{SD}) curves of each channel before and after the functionalization of olfactory nanovesicles. (e) Gating curves of CNT channels before and after the functionalization of olfactory nanovesicles.

4.5 Detection of GSM and MIB using bioelectronic nose

Figure 4.5(a) shows the real-time conductance measurement of the bioelectronic nose with different concentrations of odorants ranging from 100 pg/l to 100 μg/l. Each olfactory receptor showed dose-dependent responses to its specific ligand and the limit of detection (LOD) was 10 ng/l, which is sufficiently low level for water quality monitoring.[112] The RSD value for 10 ng/l GSM was calculated as 50.04% and 42.54% for 10 ng/l MIB (n = 3). There was no significant change after treatment with both odorants at 100 μg L^{-1}. This is attributed to the saturation of calcium ions and depletion of components for signaling within the olfactory nanovesicles.[121] The conductance change was normalized by its maximum response to calculate the sensitivity of the bioelectronic nose. Figure 4.5(b) shows the graph for the normalized sensitivity of the bioelectronic nose at different concentrations of odorants before and after functionalization of the olfactory nanovesicles. The dose-dependent responses of bioelecronic nose were analyzed by using the Langmuir isotherm model as previously reported.[24] The calculated equilibrium constant *Kd* was 3.89 x 10^8 M^{-1} with GSM and 4.00 x 10^8 M^{-1} with MIB. When nanovesicles derived from the control cells without olfactory receptors were used, no signal was observed (Figure 4.6). In a sensing system, it is very important that the sensor discriminates only the target ligand from a complex mixture. Figure 4.5(c) shows that the bioelectronic nose distinguishes GSM and MIB from other drinking water odor standards, even though much higher concentrations of control compounds were applied (Figure 4.7). To evaluate the role of calcium ions in this sensing system, the same experiments were carried out with calcium ion-free PBS buffer used as an electrolyte and no signal was observed. Furthermore, when the calcium ion channel was blocked with $MgCl_2$, the bioelectronic nose showed no responses (Figure 4(d), Figure

4.8). These results indicate that calcium flux into the nanovesicle caused a change in electrical current flow along the swCNT.

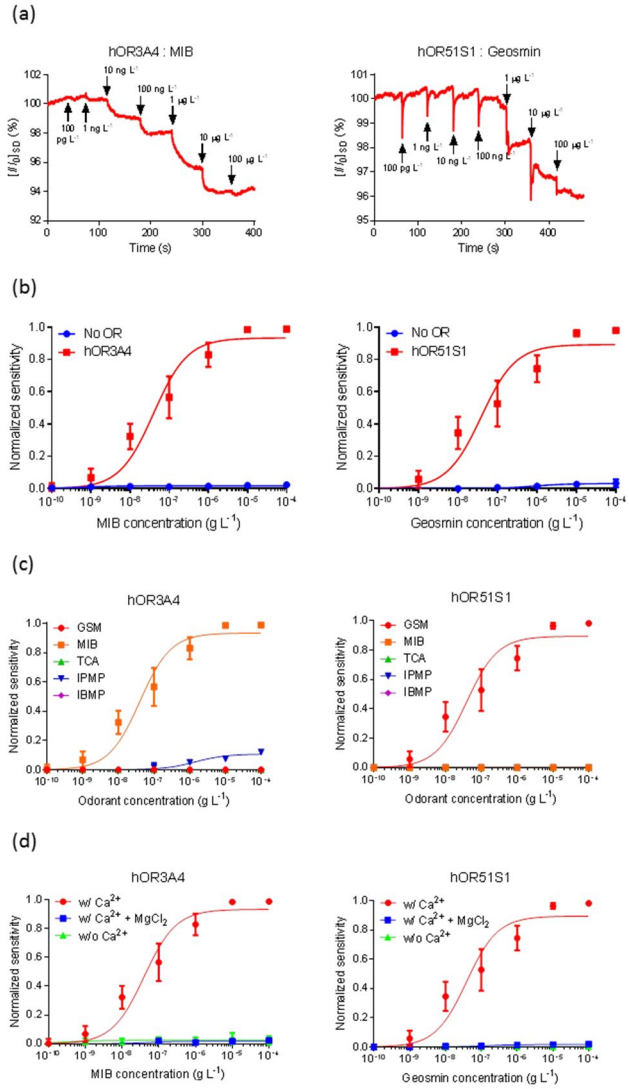

Figure 4.5 Detection of GSM and MIB using bioelectronic nose. (a) Real-time responses of bioelectronic nose to the injection of various concentrations of odorants. (b) Dose-dependent response curves of bioelectronic nose with GSM and MIB. Error bars, s. e. m. three replicates. (c) Selective responses of bioelectronic nose to GSM and MIB. (d) Effect of calcium ion and ion channel blocker on the performance of bioelectronic nose.

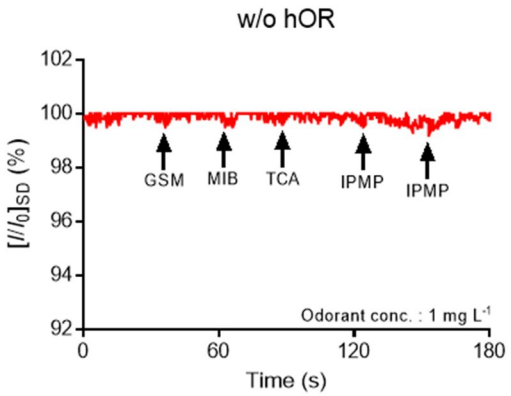

Figure 4.6 Real-time response of bioelectronic nose to each odorant without olfactory nanovesicle.

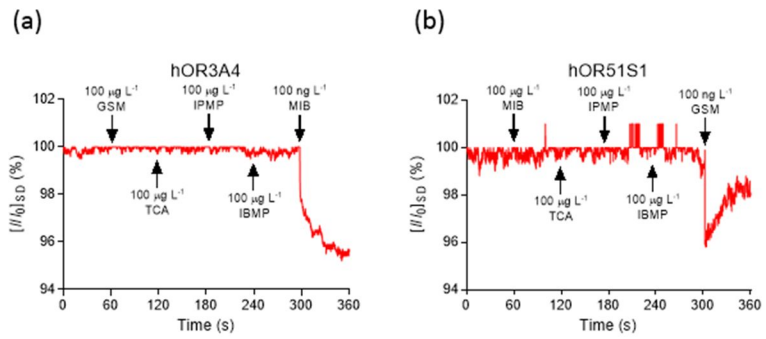

Figure 4.7 Selectivity of bioelectronic nose. (a) Selective recognition of GSM and MIB from other odorants by hOR3A4 and (b) hOR51S1-functionalized swCNT-FET.

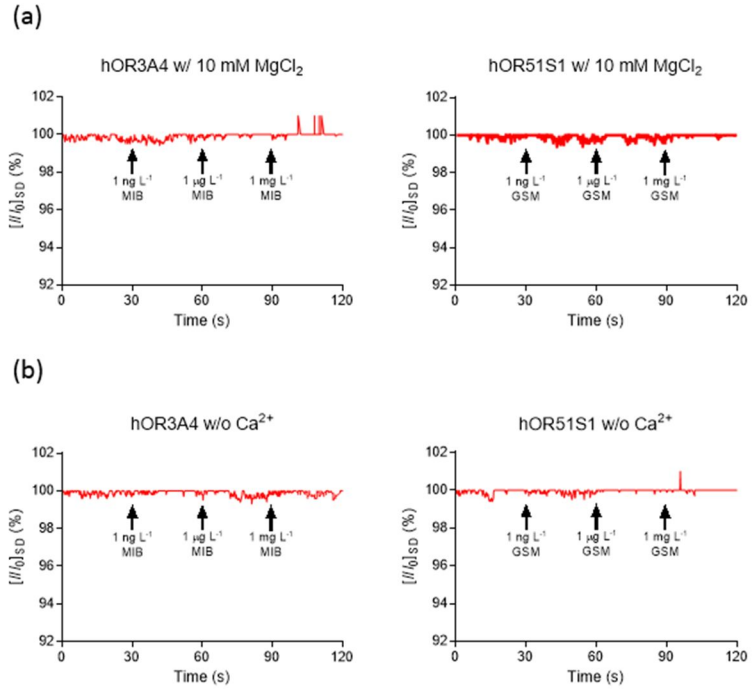

Figure 4.8 Effect of ion channel blocker and calcium ion on the bioelectronic nose. (a) Real-time response of bioelectronic nose to their specific ligand with 10 mM of $MgCl_2$, ion channel blocker and (b) without calcium ion in PBS buffer.

4.6 Detection of GSM and MIB from water samples

Water samples containing GSM and MIB were examined to evaluate whether the bioelectronic nose can be used for on-site and real-time measurement of water contamination (Figure 4.9). Each of the odorants was added to laboratory tap water, commercial bottled water (Evian, France) and river water at a concentration of 20 ng/l. The bioelectronic nose did not respond to the negative control for odorant samples, but the current signal decreased when their ligands were present in the water samples. These results indicate that the bioelectronic nose can discriminate a target ligand from water samples containing a complex mixture, and thus it can be used for fast and easy assessment of water quality without any pretreatment.

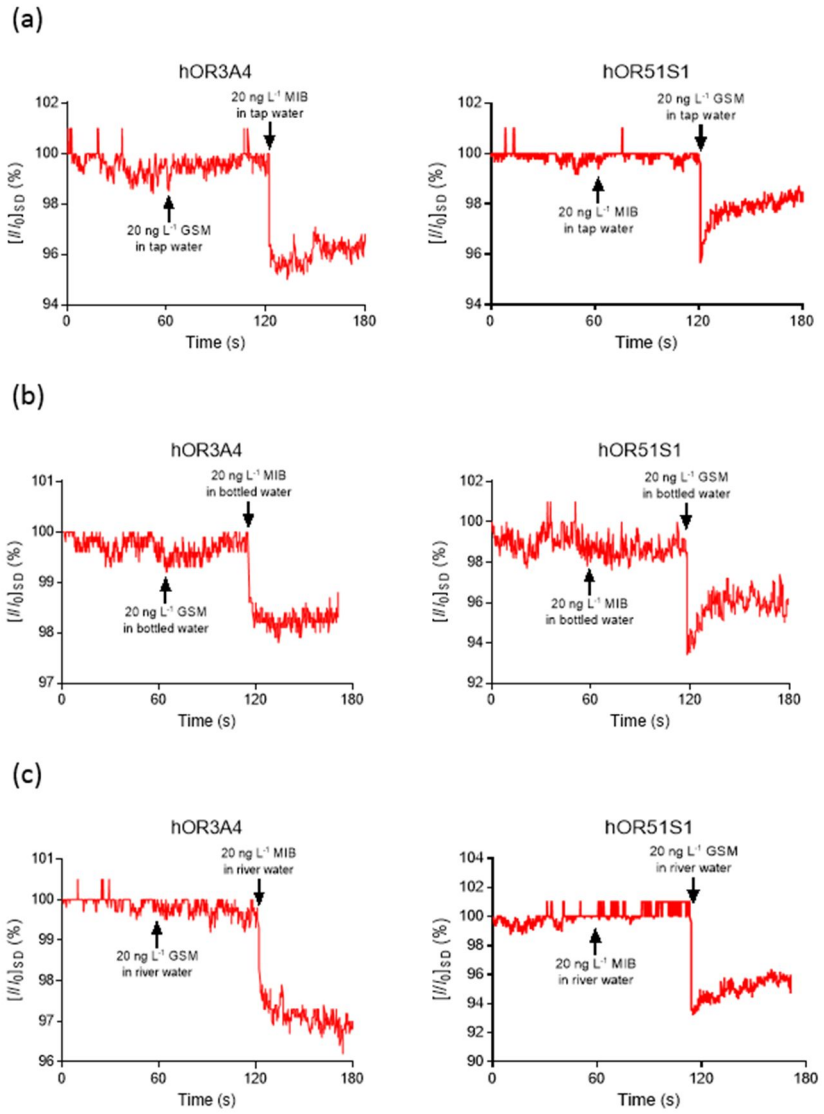

Figure 4.9 Detection of GSM and MIB from water samples. (a) Real-time recognition of GSM and MIB from tap water, (b) bottled water and (c) river water.

4.7 Conclusions

To overcome the limitations of conventional methods for rapid on-site assessment of water contamination, a bioelectronic nose was developed using human olfactory nanovesicle-functionalized swCNT-FET that mimic the human smell sensing mechanism. For the selective recognition of odor-causing molecules from contaminated water, hOR51S1 and hOR3A4 were selected as specific receptors for GSM and MIB, respectively. Olfactory nanovesicles, which were produced from mammalian cells expressing the selected hORs on the cell surface, were immobilized on swCNTs for sensitive and selective detection. The detection limit of the bioelectronic nose was at a sufficiently low level for the detection of GSM and MIB in water, supporting the application of this sensor in the assessment of water quality. And the simultaneous measurement of two odorants was available with the bioelectronic nose. Moreover, the odorants were detected in various water samples without any pre-treatment. These results clearly show that this bioelectronic nose will be suitable for the rapid and facile monitoring of water quality in real environments.

Chapter 5.

Development of bioelectronic sensor using human olfactory nanovesicles for the detection of VOCs from *in vitro* diabetic models

Chapter 5. Development of bioelectronic sensor using human olfactory nanovesicles for the detection of VOCs from *in vitro* diabetic models

5.1 Introduction

Type 2 diabetes is a severe metabolic disease which is characterized by insulin resistance, hyperglycemia, and dyslipidemia.[122] Early and exact diagnosis of diabetes is an important issue to prevent patients from serious complications such as cardiovascular disease, respiratory infection. Recently, various VOCs related to several cancers were identified with specific cells and tissues, and these VOCs were considered as biomarkers of cancers[123,124,125] and also there have been many efforts to develop the sensing system for detecting VOCs. Several studies have reported that insulin resistance in skeletal muscle and adipose tissue was induced by lipid- and fat-derived free fatty acids.[126,127] High level of free fatty acids induced inflammation resulting in glucose tolerance in muscle, heart and adipose tissue.[128,129] It is very difficult to find out biomarkers of severe diseases directly from patients although many researchers have tried to it, because there are needs for identical samples from many patients and this process is expensive, labor-intensive, and time-consuming. These difficulties can be overcome by the identification of biomarkers from *in vitro* disease cell system. Here, we identified VOCs related to diabetes using *in vitro* insulin resistant model system and developed the bioelectronic nose for detecting VOC, which selected as a biomarker of diabetes.

5.2 Construction of *in vitro* diabetes models

For the construction of *in vitro* diabetes models, mouse adipocytes (3T3-L1) and rat skeletal muscle cells (L6) were differentiated with the stimulation medium and insulin resistances were generated by the exposure to palmitic acid. Figure 5.1 (a) shows fluorescence images of glucose uptake levels of diabetes model cells. The fluorescent intensities were increased with the addition of insulin in both cells and the increased levels were returned with the addition of palmitic acid. Figure 5.1(b) shows the quantitative comparison of the glucose uptake levels. These results meant the constructed *in vitro* models had the characteristics of the early-phase diabetes models in which insulin resistance induced by free fatty acids.

SPME-GC/MS was used for the analysis of VOCs in the headspace of the diabetes models. Figure 5.2 shows GC profiles of normal and disease model of adipocytes and skeletal muscle cells. VOCs, such as ethyl 5-methylnonanoate, 17-octadecynoic acid, cis,cis-7,10-hexadecadienal were increased, and oxalic acid, 1,6,10-dodecatriene-3-carboxylic acid, cyclohexane carboxylic acid were decreased in adipocytes. In skeletal muscle cells ethyl 5-methylnonanoate, 17-octadecynoic acid (17ODYA), 12, 15-octadecadiynoic acid were increased, and dodecanoic acid, 2,5-octadecadiynoic acid were decreased. Among the analyzed VOCs, 17ODYA was selected as a biomarker for the diagnosis of insulin resistance and was used for the screening of an olfactory receptor. 17ODYA is a palmitic acid analogue and blocks leukotriene b4 hydroxylation by LTB4 hydroxylase resulting in inducing inflammation. The inflammation causes insulin resistance in muscle and adipose tissues.

(a)

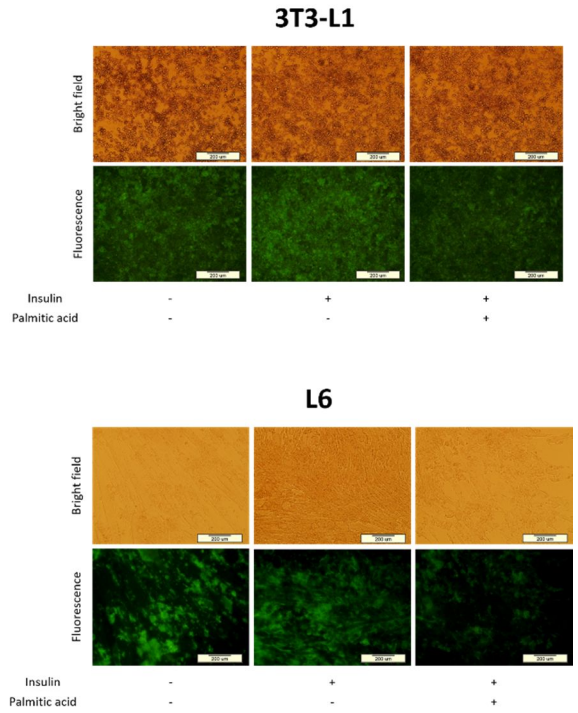

(b)

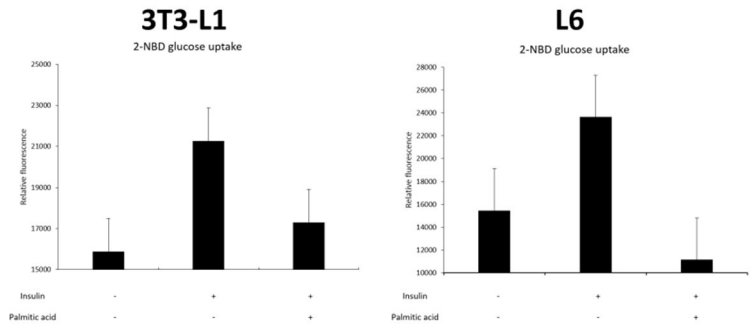

Figure 5.1 Construction of in vitro diabetic models. (a) Fluorescence images of diabetes model cells with glucose uptakes. (b) Quantitative comparison of 2-NBD glucose uptake levels of model cells.

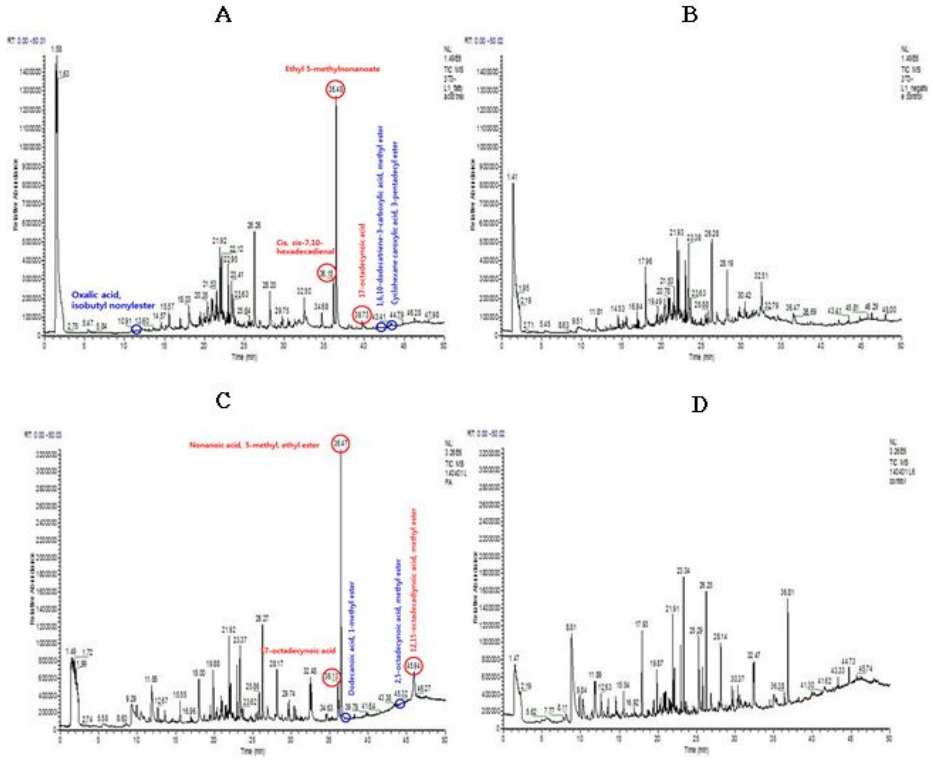

Figure 5.2 Analysis of VOCs in the headspace of diabetes model cells using SPME-GC/MS. (a) GC profiles of disease model, (b) normal adipocytes, (c) disease model and (d) normal skeletal muscle cells.

5.3 Screening of human olfactory receptors

Artificial olfactory systems were constructed for the screening of human olfactory receptors which can selectively recognize 17ODYA for the diagnosis of insulin resistance. Human ORs and accessory proteins were co-transfected to HEK-293 cells, and CRE-luciferase reporter gene assay was performed. We stimulated 86 hORs with 1 mM 17ODYA in triplicate (Figure 5.3(a)), and the specificity of the responded receptors was tested with cancer biomarkers such as 1,3-dichlorobenzene (MDCB), 2-ethyl-1-hexanol (2E1H) and hexanal (HEX) (Figure 5.3(b)). As results, OR51A4 was selected as the specific receptor for the development of the bioelectronic nose. Cell surface expression of hOR was analyzed by immunocytochemistry (Figure 5.3(c)).

(a)

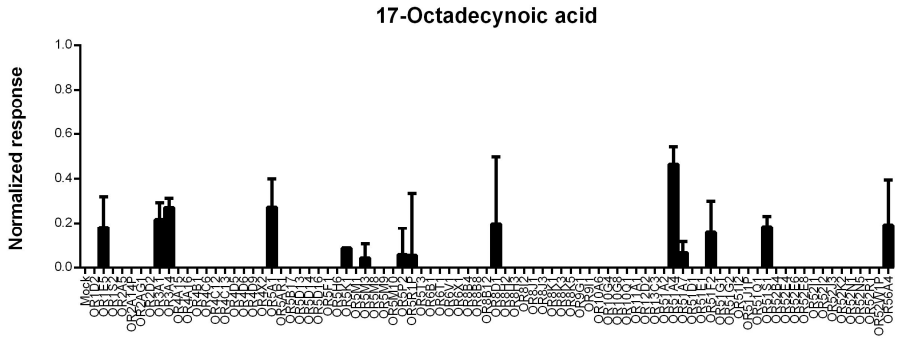

(b)

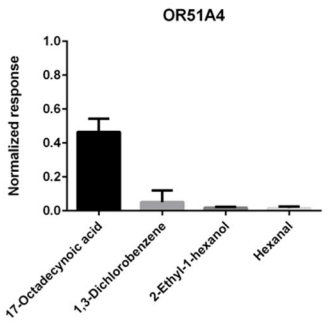

(c)

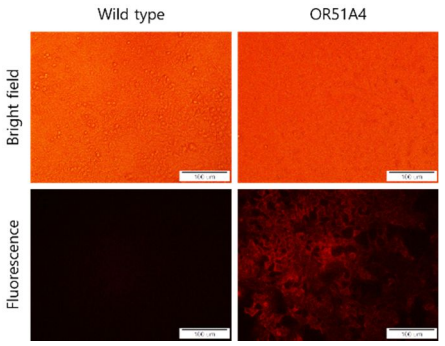

Figure 5.3 Screening of human olfactory receptors. (a) Responses of 86 human olfactory receptors to 17ODYA. (b) Selectivity of OR51A4. (c) Immunocytochemistry of OR51A4 in HEK-293 cells.

5.4 Construction of nanovesicle-based bioelectronic nose

For the scalable integration of human olfactory receptor onto CNT-FET, nanovesicles were produced as described in chapter 4.3. The diameter of nanoveislces was approximately 100 nm (Figure 5.4(a)). OR51A4 existed in hOR expressing cell-derived nanovesilces (Figure 5.4(b)). The functionality of OR51A4 in nanovesicles was analyzed by calcium assay with fluorescent dye (Figure 5.4(c). Only nanovesicles containing OR51A4 have the binding ability with 17ODYA.

CNT-FET was fabricated via the photolithography method and CNT channels were incubated with positively charged PDL. Nanovesicles which have negative charges at the surface were immobilized onto PDL-coated CNT channels (Figure 5.5(a)). Source-drain current-voltage relationships before and after the nanovesicle immobilization were analyzed to identify the electrical properties of the bioelectronic sensor. Although the resistance was increased, the linearity of the curve was sustained, and stable ohmic behavior was observed (Figure 5.5(b)). Figure 5.5(c) shows a liquid ion gate profiles of the CNT-FET before and after the nanovesicle immobilization. Clear p-type behavior was maintained and these electrical properties indicated that the nanovesicle-based bioelectronic sensor can be used for the detection of 17-ODYA.

(a)

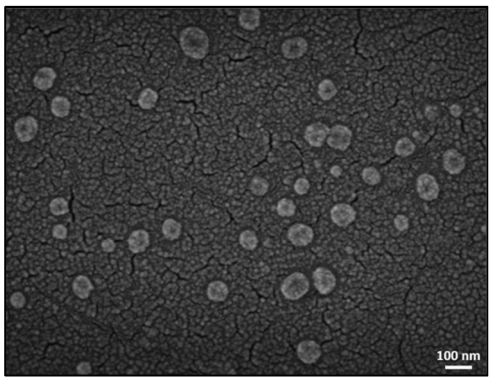

(b)

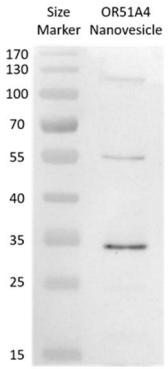

(c)

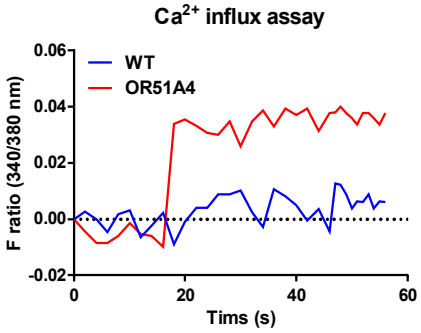

Figure 5.4 Characterization of olfactory nanovesicles. (a) SEM image of nanovesicles. (b) Western blot analysis of OR51A4 in nanovesicles. (c) Calcium influx assay of nanovesicles with the addition of 1mM 17ODYA.

(a)

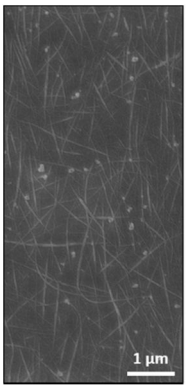

(b)

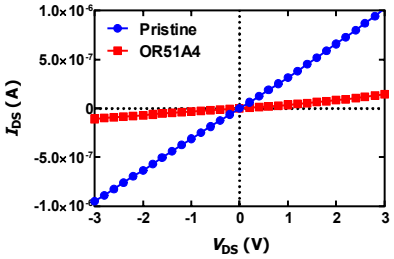

(c)

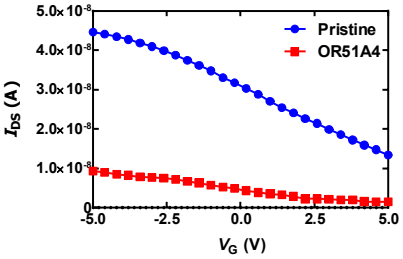

Figure 5.5 Characterization of nanovesicle-based bioelectronic nose. (a) SEM image of nanovesicle-immobilized CNT channels. (b) current-voltage curves and (c) gating curves of CNT channels before and after the immobilization of olfactory nanovesicle.

5.5 Detection of 17ODYA using bioelectronic nose

Figure 5.6 (a) shows the real-time current changes of the bioelectronic nose with concentrations of 17ODYA from 1 fM to 1 pM. Only olfactory nanovesicle nanovesicle-functionalized CNT-FET showed dose-dependent responses to 17ODYA. Figure 5.6 (b) shows the normalized sensitivity of the bioelectronic nose at different concentrations of 17ODYA before and after the immobilization of olfactory nanovesicles, and the detection limit of the bioelectronic nose was 10 fM. Figure 5.6(c) and (d) show the selective detection of 17ODYA against other cancer markers such as MDCB, 2EH1 and HEX. These results indicated that the bioelectronic nose functionalized with OR51A4 can selectively detect the diabetes biomarker and could be used for the rapid and simple diagnostic tool for diabetes.

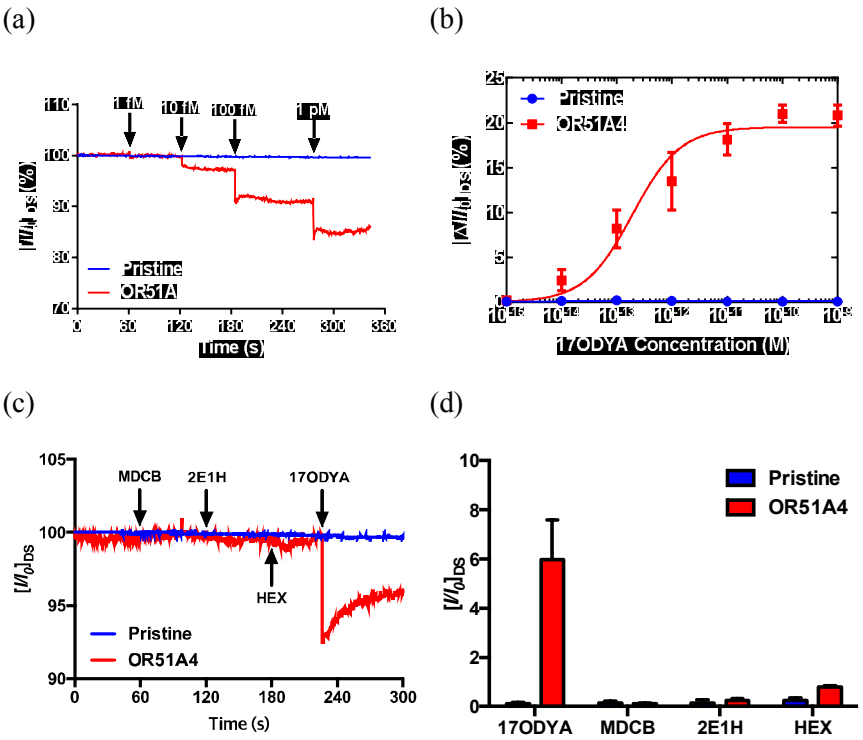

Figure 5.6 Detection of 17ODYA using bioelectronic nose. (a) Real-time responses and (b) normalized sensitivity of the bioelectronic sensor with various concentrations of 17ODYA. (c) Real-time responses (d) selective responses of the bioelectronic sensor to biomarkers before and after the olfactory nanovesicle immobilization.

5.6 Conclusions

Here we constructed the *in vitro* models of diabetes by inducing insulin resistance in mouse adipocytes and skeletal muscle cells. Volatile organic compounds from the headspace of *in vitro* models were identified using the SPME-GC/MS methods. 17ODYA was increased in both model cells and selected as the potential biomarker of diabetes. Human olfactory receptor was screened for the selective recognition of diabetes biomarker, produced as nanovesicles for the scalable integration with the CNTs. The bioelectronic nose was developed for the diagnosis of diabetes using an olfactory nanovesicle and a CNT-FET. The bioelectronic nose could detect 10fM of 17ODYA in dose-dependent manner and selectively discriminate the target odorant from other odorants. This approach can be used as a useful tool for developing bioelectronic noses for diagnosis of various diseases that biomarkers are not identified.

Chapter 6.

Development of portable and multiplexed bioelectronic sensor using human olfactory and taste receptor proteins for the assessment of food quality

Chapter 6. Development of portable and multiplexed bioelectronic sensor using human olfactory and taste receptor proteins for the assessment of food quality

6.1 Introduction

To overcome the limitations of conventional analytical methods, highly sensitive and selective bioelectronic sensors that mimics the human olfactory/taste system have been developed.[49,130,131] The sensors use olfactory or taste receptors as primary recognition molecules and nanomaterials such as carbon nanotube, [24,25,85,86,89,90,91,92,93,94,104,118,] conducting polymer[88,105] and graphene[87,95] as secondary transducers for signal amplification from the primary recognition molecules. The sensors have both the advantage of the high selectivity of a natural system and the high sensitivity of a nanomaterial-based electronic sensor. These sensors can be applied to the analysis of food quality,[91,92,93,94,105] disease diagnosis[89], and environmental assessment.[90]

Although the sensors distinguish their target molecules with high resolution, they cannot recognize complex mixtures like humans perceive. The human olfactory and taste systems are activated by the combinatorial pattern recognition of various receptors.[81,132,133] For an accurate representation of the human olfactory/taste system and simultaneous analysis of various odors and tastes, multiplexed sensing systems are required with different kinds of receptors. In our previous work, the size of the sensor was small enough, but the size of the measurement equipment was not small enough for on-site analysis. Thus, in addition to multiplexed sensing, miniaturization of the monitoring system is necessary for practical on-site application of the bioelectronic sensor.

Herein, we developed a portable and multiplexed bioelectronic sensor that combines human olfactory and taste receptors with a multi-channel

CNT-FET, which can be used to obtain comprehensive information regarding food freshness from various viewpoints. For the multiplexed analysis of taste- and odor-causing compounds produced by food, four different kinds of receptors were produced in *E. coli*[134] and their structures and functional properties were confirmed. The recombinant receptors were immobilized onto CNT channels with a uniform orientation using a nickel-histidine reaction. The CNT-FET sensor was designed as a 4 x 4 multi-channel type, and all channels were divided by microwells fabricated by 3D printing technology. For on-site application, a conventional portable monitoring system was customized for the multi-channel type bioelectronic sensor, which was operated by a laptop computer. The device successfully distinguished the four different molecules, and the pattern recognition of complex mixtures was available by the binding of target molecules to their specific receptors without any interference from other non-target molecules in the mixture. This allowed a successful analysis of various aspects of food quality.

6.2 Expression, purification, and refolding of human sensory receptors

For the detection of taste and odor molecules, four different kinds of olfactory and taste sensory receptors were selected; OR2J2 and OR2W1 for octanol, OR2W1 for hexanal,[135] TAAR5 for trimethylamine[136] and TAS2R38 for goitrin.[137] These taste and odor molecules are indicators of food contamination; octanol for bacterial contamination in beef,[138] hexanal for lipid oxidation in dairy products,[139,140] trimethylamine for seafood decomposition,[141] and goitrin for antithyroid toxin in vegetables.[137] The receptor genes were amplified from human genomic DNA and cloned into pET-DEST42, a bacterial expression vector. A 6xHis-tag was fused to the C-terminus of the receptor proteins for purification and oriented

immobilization on the Ni-coated CNTs. The receptor proteins were expressed as inclusion bodies in *E. coli* BL21 (DE3) and solubilized with SDS and DTT. They were purified with a His-tag gravity column using pH gradient method and reconstituted using a detergent micelle method to maintain the original structure of the receptor proteins.

Figure 6.1(a) shows the SDS-PAGE images of the produced and purified proteins. All receptor proteins were successfully expressed withat the expected size and purified at high purity. Western blotting was carried out using an antibody against the His-tag to confirm its fusion to the receptor proteins (Figure 6.1(b)). Their secondary structures were analyzed by circular dichroism spectroscopy. Human olfactory and taste receptors are mainly composed of alpha helices and possess strong negative bands at 208 and 220 nm of wavelength.[135,142,143] Figure 6.1(c) shows that all reconstituted proteins had minimal values at both the predicted wavelengths, indicating that they were well-constructed through the reconstitution process. The functionality of the proteins was evaluated using a tryptophan fluorescence quenching method (Figure 6.1(d)). The fluorescence of proteins is mainly due to the excitation of tryptophan residues, and conformational changes in proteins upon ligand binding decreases the fluorescence intensity by shielding the tryptophan residues.[144] In the present study, the selected sensory proteins contain several tryptophan residues; five residues in OR2J2, three residues in OR2W1, eight residues in TAAR5, and nine residues in TAS2R38. Fig. 1d shows that the receptor proteins selectively recognize their ligands in a dose-dependent manner. This indicates that the produced proteins have the specificity of the human sensory systems and could be used as primary recognition elements of the bioelectronic sensor.

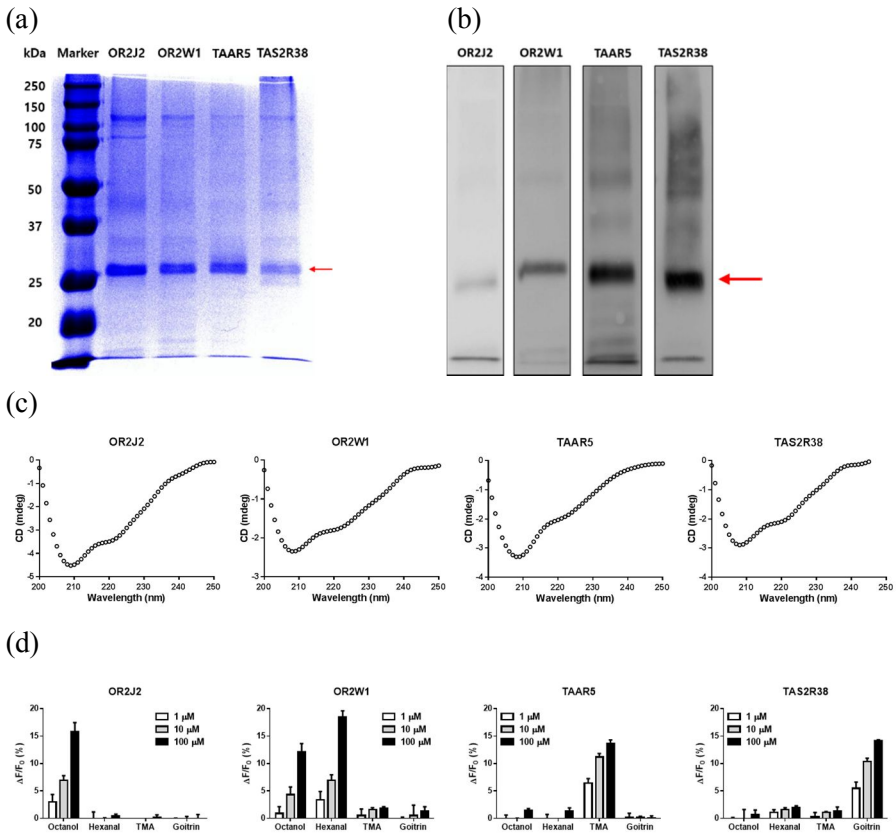

Figure 6.1 Functional production of human olfactory and taste receptors. (a) SDS-PAGE and (b) Western blotting analysis of purified and reconstituted receptor proteins; olfactory receptors OR2J2, OR2W1 and TAAR5, and taste receptor TAS2R38. (c) Secondary structure analysis of olfactory and taste receptor proteins. (d) Evaluation of the receptor selectivity with octanol, hexanal, trymetylamine and goitrin. Error bars, SD, triplicate.

6.3 Fabrication of multi-channel bioelectronic sensor

Figure 6.2(a) is a schematic diagram representing the fabrication process of a multi-channel sensor (MCS) and channel splitter. The MCS was fabricated using a previously reported method (detailed in Materials and Methods).[24,89,104] Briefly, the electrodes and channels were patterned onto an SiO_2 wafer via the photolithography method, and the patterned wafer was incubated in SWCNT solution. A passivation layer was created on the electrodes to prevent the leakage of current under aquatic conditions. The fabricated MCS had four quadrants, each composed of four compartmentalized CNT network channels. The CNT network channels were functionalized with an Ni component for immobilization of the four types of receptors using a method reported in previous papers.[118,145] The MCS was incubated in 4-carboxybenzene diazonium tetrafluoroborate solution to functionalize the SWCNTs on the channels. Subsequently, the carboxylic acid of the 4-carboxybenzene was activated in activation buffer and was immersed in N ,N -bis(carboxymethyl)-L-lysine hydrate (NTA-NH_2) solution. Finally, the MCS was washed with deionized water and placed in a solution of $NiCl_2$ for the functionalization of Ni^{2+} on SWCNTs.

A channel splitter was fabricated using a 3D printer, and designed with the different wall heights to prevent various solutions from mixing with each other. The wall inside the quadrant (X-shaped walls) plays a role in splitting the inner part of the MCS, preventing one receptor solution from mixing with another during the receptor immobilization process. The outer wall helps to set a consistent solution volume on the channel parts and block the solution from contacting the pads. The channel splitter was coated with a thin layer of polydimethylsiloxane (PDMS) to prevent the leakage of solutions, and was fixed on the channel part of the MCS. The assembled MCS was baked at 120 °C for 30 min to cure the PDMS.

Figure 6.2(b) and (c) are optical images of the MCS with the channel splitter. Each quadrant is composed of four CNT network channels, each of which has 160 individual parallel CNT network lines (indicated by the yellow arrows in Figure 6.2(d). The CNT networks were laid out in an interdigitated shape to minimize the size of the sensor. Figure 6.2(d) shows an atomic force microscopy (AFM) image of parallel CNT network lines. The length and width of one CNT network line are 100 μm and 3 μm, respectively. In a multiplexed sensing system, the deviation of device characteristics plays an important role in data analysis. Figure 6.3 shows the effect of the CNT network line number on the deviations of device characteristics. Each value was averaged from sixteen devices for data analysis. The graphs show that deviations decreased as the number of CNT network line increased. For 160 CNT network lines, the deviations of device characteristics decreased to 30% compared with 40 CNT network lines. This result indicates that the large number of CNT network lines decrease the variation among numerous sensor devices and enhance the reliability of sensor performance.

We investigated the characteristics of pristine MCSs and various receptors-immobilized MCSs using AFM. Figure 6.2(e) shows AFM topography images prior to and following receptor immobilization on CNT network channels. We measured AFM images in tapping mode with a scan rate of 0.4 Hz for pristine CNT channels. Following imaging of pristine CNT networks, receptors were immobilized on the channels and the AFM image was scanned at the same location of the channel, with a scan rate of 0.1 Hz to avoid unintended noise signals from sticky biomolecules. Figure 6.2(e) shows cross-section profiles on the horizontal lines of the upper AFM images. The heights of the CNT networks increased following immobilization of receptors, especially at some prominent peak points. Following the immobilization of OR2J2, OR2W1, TAAR5, and TAS2R38 on the CNT networks, the heights were increased by approximately 1.94,

1.82, 2.82, and 1.74 nm, respectively, compared with the pristine ones. The increased heights are considered to be evidence of successful receptor immobilization on the CNT networks.

Figure 6.2(f) shows the electrical characteristics of MCSs prior to and following the immobilization of four types of sensory receptor on the CNT network channels. We measured characteristics I-V and liquid gate profiles of MCSs using a semiconductor analyzer. The blue and red lines are the electrical characteristics of the pristine and receptor-immobilized MCSs, respectively. The graphs show the formal p-type semiconductor characteristics regardless of receptor immobilization, indicating that receptor immobilization on the CNT networks does not significantly affect the characteristics of MCSs.

(a)

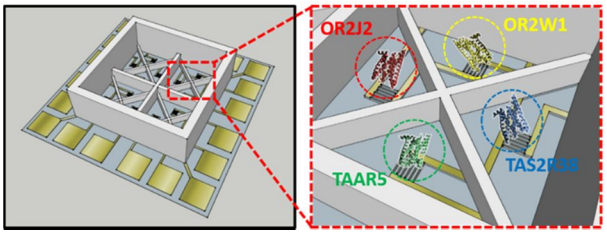
OR2J2
OR2W1
TAAR5
TAS2R38

(b) (c) (d)

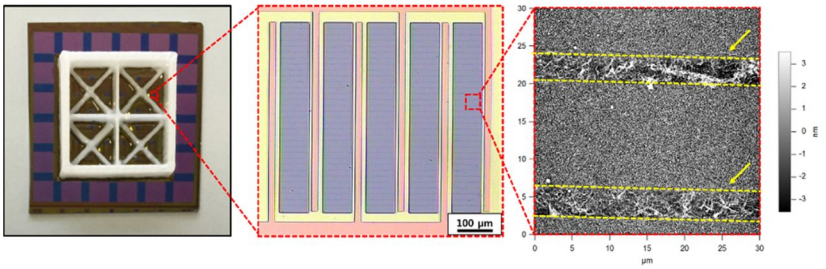
100 μm
μm
nm

(e)

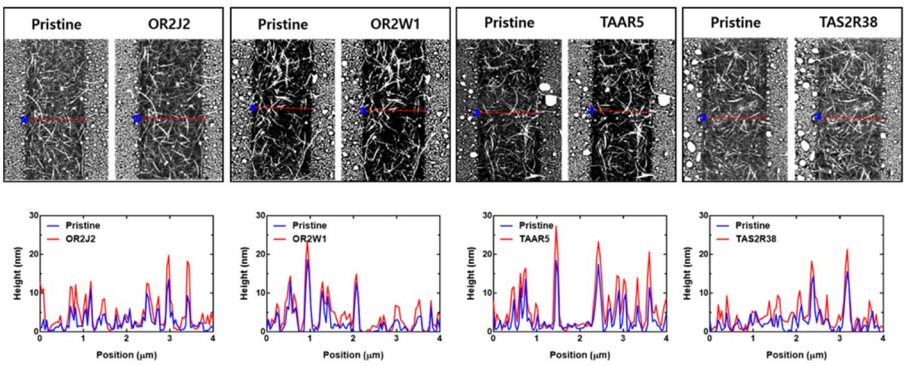
Pristine
OR2J2
Pristine
OR2W1
Pristine
TAAR5
Pristine
TAS2R38
Height (nm)
Position (μm)

(f)

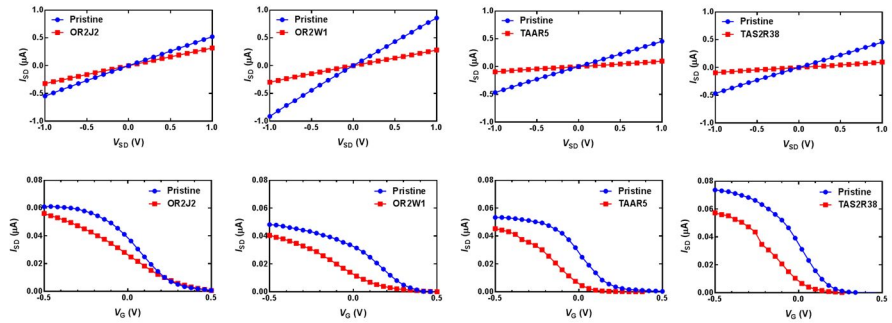

Figure 6.2 Fabrication and characterization of a multi-channel CNT-FET sensor. (a) Schematic diagram of an olfactory and taste receptor-functionalized multi-channel-type CNT-FET platform. (b) Optical image of a multi-channel-type CNT-FET and (c) CNT channels. (d) SEM image of CNT channels. (e) AFM images and height profiles of CNT channels prior to and following functionalization with receptors. (f) Current-voltage curves and gate profiles of CNT channels prior to and following functionalization with receptors.

(a) (b) (c)

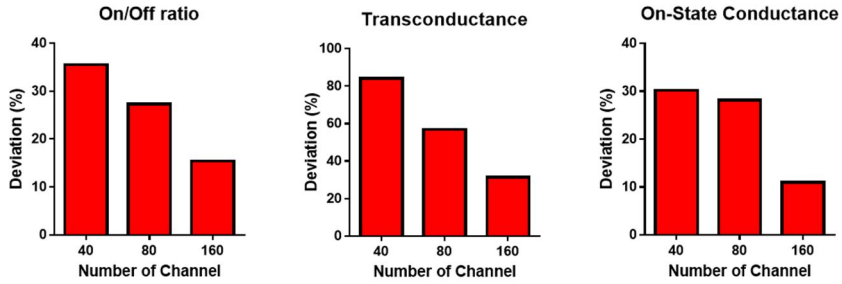

Figure 6.3 Effect of the channel number on the standard deviations of multi-channel CNT properties. (a) On/off ratio, (b) transconductance and (c) on-state conductance.

6.4 Detection of odor and taste molecules using bioelectronic sensor

We also developed a customized portable measurement system for the detection of various molecules using the MCSs (Figure 6.4(a)). The portable system is composed of 20 probes, a 16-to-1 multiplexer and a microcontroller unit to switch from one channel to another. A HyperTerminal was used as the platform for instrument control. We applied bias voltages of 0.1 V to the reference pads and measured the current signals with a resolution of 10^{-10} A. 16 probes were utilized for the measurement of conductance changes, and the other 4 probes were used as the reference pads. The channels were switched sequentially from 1 to 16, and repeated 3 times. This platform was designed to be connected to a laptop computer via a USB cable for its portable application. When odor and taste molecules were injected into the multi-channel-type CNT, the receptor-functionalized channel showed conductance changes with high selectivity (Figure 6.4(b)). There were no significant changes in conductance at the pristine CNT channels (Figure 6.5). The change in conductance was normalized to the maximum response, and Figure 6.4(c) shows the normalized sensitivity and distinguishing ability of the sensor at different concentrations of specific target molecules. The dose-dependent signals were analyzed with the Langmuir isotherm and the calculated K_d values were 7.53 x 10^{12} M^{-1} for OR2J2 and octanol, 3.05 x 10^{10} M^{-1} for OR2W1 and octanol, 2.31 x 10^{11} M^{-1} for OR2W1 and hexanol, 1.97 x 10^{11} M^{-1} for TAAR5 and trimethylamine, and 1.782 x 10^{12} M^{-1} for TAS2R38 and goitrin. The human olfactory system is known to recognize a smell by the sum of receptor binding, and antagonistic interactions of olfactory receptors have been reported,[146] thus, interference effects between the receptors and odor molecules were examined. When we compared the electrical signals of each target molecule and the target molecules in mixtures, non-target

molecules in the mixture did not affect the electric signal and intrinsic signals of the target molecules were obtained even in the mixtures. (Figure 6.4(d)) These results show that the target molecule can be detected selectively without any interference from other non-target molecules in the complex mixture.

(a)

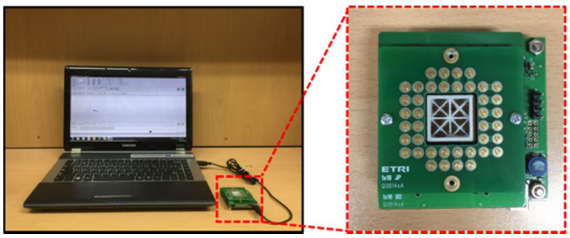

(b)

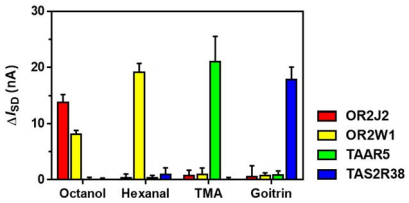
30
20
10
0
ΔISD (nA)
Octanol
Hexanal
TMA
Goitrin
OR2J2
OR2W1
TAAR5
TAS2R38

(c)

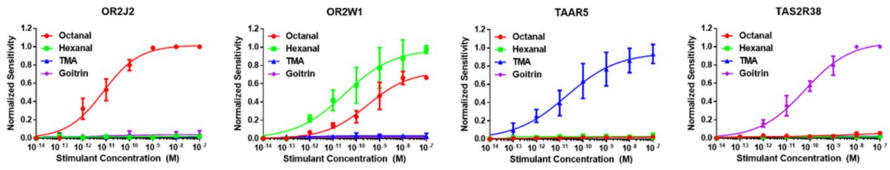
OR2J2
OR2W1
TAAR5
TAS2R38
Octanal
Hexanal
TMA
Goitrin
Normalized Sensitivity
Stimulant Concentration (M)

(d)

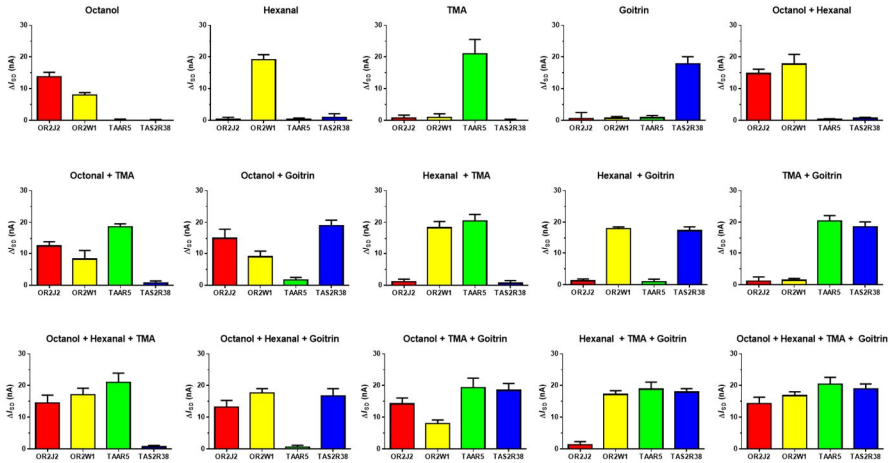
Octanol
Hexanal
TMA
Goitrin
Octanol + Hexanal
Octonal + TMA
Octanol + Goitrin
Hexanal + TMA
Hexanal + Goitrin
TMA + Goitrin
Octanol + Hexanal + TMA
Octanol + Hexanal + Goitrin
Octanol + TMA + Goitrin
Hexanal + TMA + Goitrin
Octanol + Hexanal + TMA + Goitrin
ΔISD (nA)
OR2J2
OR2W1
TAAR5
TAS2R38

Figure 6.4 Detection of target molecules using a customized monitoring platform. (a) A photograph of the portable and multiplexed bioelectronic sensor connected to a laptop computer. (b) Signal pattern recognition of each odor and taste molecule by the bioelectronic sensor (the concentrations of target molecules were fixed at 1 nM). (c) Normalized sensitivity of the sensor based on each sensory receptor. (d) Signal pattern recognition of each target molecule and target molecules in complex mixtures. Error bars, SD, triplicate.

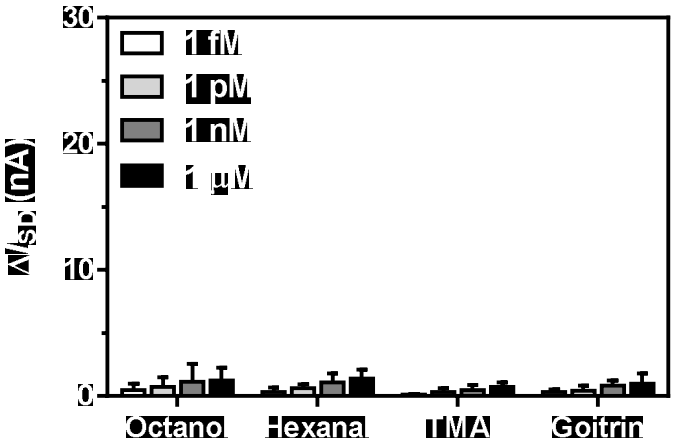

Figure 6.5 Responses of pristine CNT-FET to octanol, hexanal, trimethylamine and goitrin.

6.5 Assessment of food freshness using biolelectronic sensor

Food is the major source of human nutrition in order to maintain a healthy life. Nobody wants to eat stale food, and consumption of contaminated food can lead to serious diseases, therefore, it is important to control food quality in various food industries.[147] There are many conventional methods for the assessment of food quality; 1) physical (viscosity, chromaticity, turbidity, solubility), 2) physicochemical (moisture, acid value, sugar content, nutritional content analysis), 3) microbiological challenge (bacterial counts) method, and 4) human sensory test (appearance, flavor, taste, texture).[148] However, these methods are not suitable for rapid analysis due to their invasive and complex pretreatment steps, long analytical times and requirement for an expert. To overcome the limitations of the conventional methods, we applied our bioelectronic sensor to the assessment of food quality. Since our target molecules, such as octanol, hexanal, trimethylamine, and goitrin, are known to be indicators of food contamination, it was expected that we would detect these molecules in various kinds of foods, therefore we measured the response of the bioelectronic sensor to treatment with several food samples. Various food samples were stored in a refrigerator and analyzed by the bioelectronic sensor every day (Figure 6.6). Among the prepared food samples, banana, strawberry, potato, and chicken did not induce any significant current changes in the sensor. However, in the case of beef and pork samples, a signal change was observed in the OR2J2-functionalized channel after 3 days, and in the OR2W1-functionalized channel after six or seven days. In the case of cheese and milk, the octanol concentration increased after two days. Trimethylamine began to be detected from both oyster and shrimp after day one and day three, respectively. Goitrin, which is an antithyroid toxin, was observed in broccoli and cabbage. Interestingly, the signal

intensity induced by broccoli and cabbage did not increase with storage time and was steadily maintained from day zero to day seven. These results indicate that our sensor can be effectively used for simultaneous analysis of food freshness from various viewpoints.

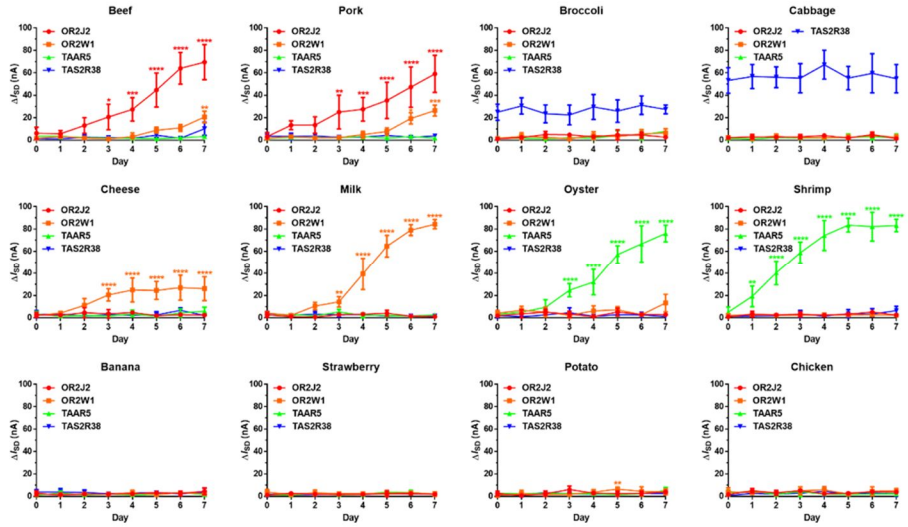

Figure 6.6 Signal pattern analysis of various food samples. Error bars, SD, three replicates. (*$P < 0.05$, **$P < 0.01$, ***$P < 0.001$, ****$P < 0.0001$)

6.6 Conclusions

In the present study, by the integration of human olfactory/taste receptors to the multi-channel CNT-FET platform with channel splitter, we developed a portable and multiplexed bioelectronic sensor for the simultaneous detection of the target molecule in the mixtures. The sensing device selectively distinguished mixtures of these molecules as well as individual odor and taste molecules with high sensitivity, and became portable by combining the miniaturized current measurement system with the carbon nanotube so that electrical signals can be rapidly analyzed in the field in real-time. From our results, it is expected that this multiplexed bioelectronic sensor can be used as a useful tool for the quality assessment of various foods and for diverse on-site detection of various molecules by applying other olfactory and taste receptors to this sensing platform.

Chapter 7.

Development of peptide-based bioelectronic sensor using extracellular loops of aquaporin for the diagnosis of neuromyelitis optica

Chapter 7. Development of peptide-based bioelectronic sensor using extracellular loops of aquaporin for the diagnosis of neuromyelitis optica

7.1 Introduction

Neuromyelitis optica (NMO, also known as Devic's disease) is a severe and uncommon disease of the central nerve system (CNS) that principally attacks the optic nerves and spinal cords.[149,150] The symptoms of the disease, including blindness and paralysis, are very serious. NMO is commonly confused with multiple sclerosis (MS) because the symptoms are similar. Since the treatments for the two diseases are different, an accurate diagnosis in the early phase is important. In 2004, NMO-IgG was found to be a highly specific biomarker in human blood and enabled the differentiation of NMO and MS patients.[151,152] This disease's specific antibody targets aquaporin-4 (AQP4), a transmembrane protein expressed in the CNS, that regulates water transport in astrocytes and ependymal cells. Various laboratory tests using AQP4 were developed for the detection of AQP4 antibody with tissue-, cell- and protein-based assays.[153,154,155,156,157,158,159,160] However, these methods have the limitations such as low sensitivity and long analytical time for diagnosis.

In a recent study, three extracellular loops (A, C and E) of AQP4 were found to contain disease-specific epitopes, which could be used in an assay for the diagnosis of NMO.[161,162] In order to overcome the drawbacks of existing methods, we propose a peptide-based CNT biosensor for the rapid detection of AQP4 antibody in human serum. A CNT-based FET has been used for the rapid detection of biological molecules with high sensitivity. CNTs have a large surface to volume ratio due to their unique one-dimensional nanoscale structures. Thus, the electrical properties of CNTs could be easily changed by adsorptions of biomolecules onto their surfaces.

We synthesized AQP4 extracellular loop peptides and directly immobilized them onto CNT channels. Using this biosensor, we could detect AQP4 antibody, a biomarker of NMO disease, with a detection limit of 1 ng/l. Furthermore, the sensor was able to detect the antibody without any pretreatment of the human serum.

7.2 Construction of peptide-based bioelectronic sensor

Three kinds of AQP4 extracellular loop peptides were synthesized, and three molecules of phenylalanine (Phe) were added to the C-terminus in order to immobilize the synthesized peptides onto CNTs via pi-pi interactions between CNTs and the aromatic rings of Phe.[12,13] In order to have a maximal capacity for antibody sensing, sufficiently high concentrations of the peptides were immobilized on the CNT channels as a monolayer via self-assembly and unbounds were washed away with distilled water. The fabricated CNT biosensor could detect AQP4 antibody, which had a p*I* value of 9-10 and was positively-charged in PBS of pH 7.4, with a decreased conductance. Figure 7.1 shows the sensing mechanism of the AQP4 loop peptide-based biosensor.

To confirm the immobilization of the peptides, an AFM image analysis was performed. Figure 7.2(a) shows the AFM images of the CNT channels before and after the immobilization of three kinds of AQP4 extracellular loop peptides. When we compared the height profiles of specific CNT regions, the height was increased by 0.71 ± 3.13 nm with AQP4 loop A, 0.56 ± 2.9 nm with AQP4 loop C and 1.4 ± 2.9 nm with AQP4 loop E (Figure 7.3(b)). These results show a successful immobilization of the AQP4 extracellular loop peptides on CNT channels.

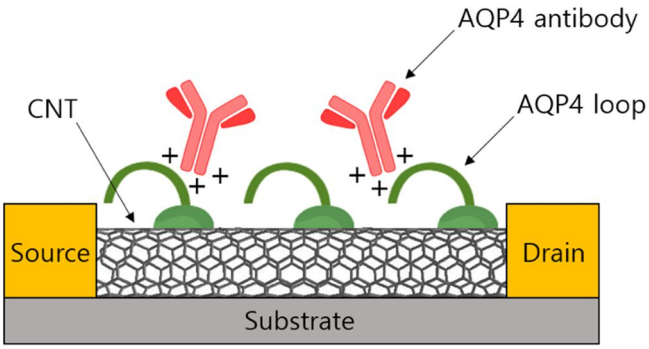

Figure 7.1 Schematic diagram showing the sensing mechanism of an AQP4 loop peptide-based CNT-FET biosensor. Positively-charged AQP4 antibody binds with the AQP4 extracellular loop peptides on CNTs, which gives a positive field-effect on the FET and decreases its electric conductance.

(a) (b)

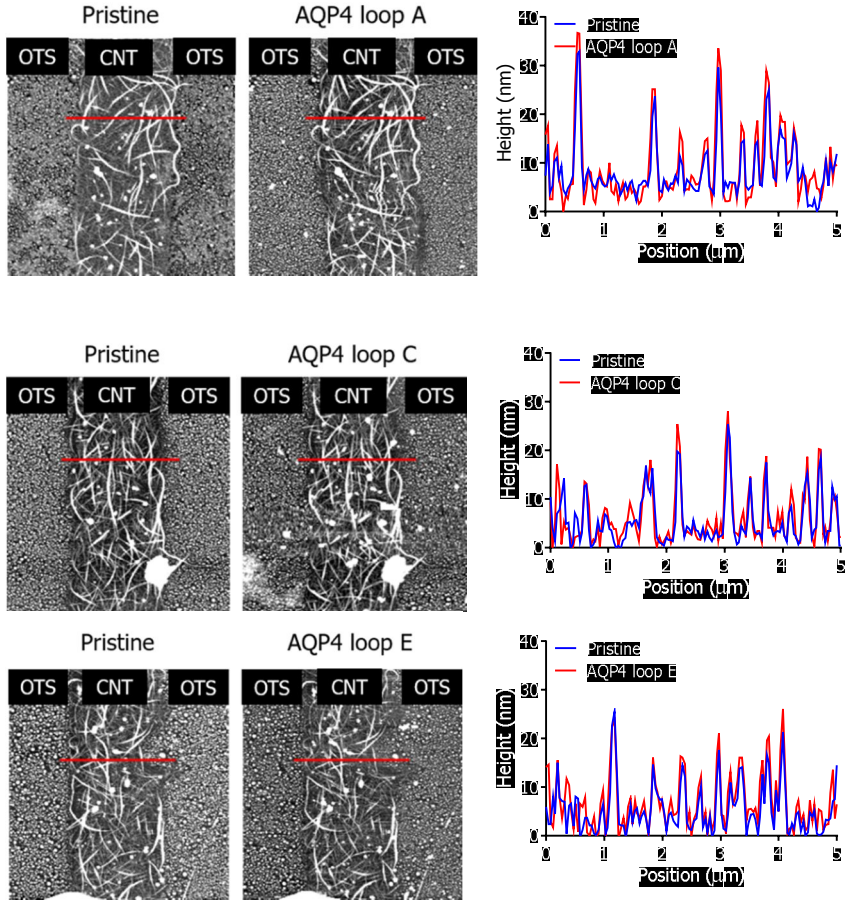

Figure 7.2 Immobilization of peptides onto the CNT channels (a) AFM images of a CNT channel before and after the immobilization of AQP4 extracellular loop peptides. (b) Comparison of measured height profiles of CNT channels before (blue line) and after (red line) the immobilization of peptides.

7.3 Electrical characteristics of peptide-based bioelectronic sensor

To evaluate the electrical property of the biosensor, the source-drain current-voltage (I_{SD}-V_{SD}) of CNT channels was measured (Figure 7.3(a)). Although the resistance of the FET sensor was increased from $6.55 \times 10^5\,\Omega$ to $1.54 \times 10^6\ \Omega$ with AQP4 loop A, $6.57 \times 10^5\ \Omega$ to $1.23 \times 10^6\ \Omega$ with AQP4 loop C and $6.59 \times 10^5\ \Omega$ to $1.11 \times 10^6\ \Omega$ with AQP4 loop E, the linearity of the curve was maintained before and after the immobilization of the peptides. We constructed a liquid-ion gated FET system with PBS (pH7.4). The source-drain current of the CNT channel was measured while increasing the gate voltage (Figure 7.3(b)). The current between the source and the drain (I_{SD}) decreased with an increasing gate voltage (V_G), indicating p-type FET behavior. These electrical characteristics indicate that the sensor can detect positively-charged AQP4 antibody in PBS.

(a) (b)

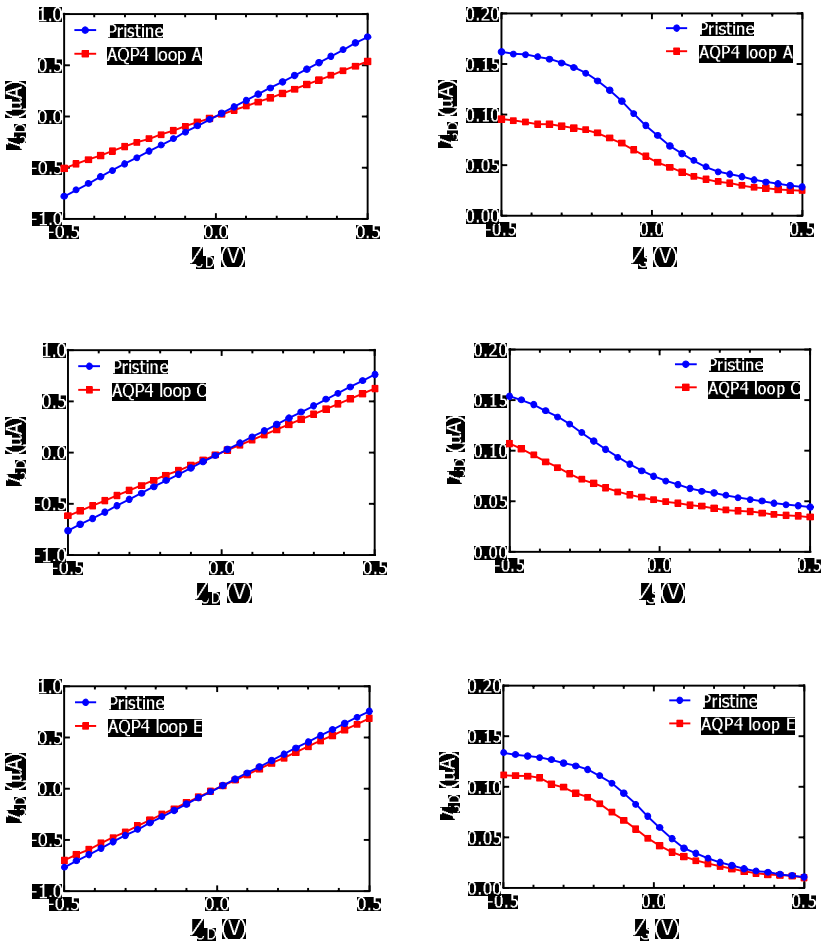

Figure 7.3 Electrical characteristics of peptide-based bioelectronic sensor. (a) Current-voltage curves and (b) Gate profiles of the CNT-FET before (blue line) and after (red line) the functionalization of AQP4 loop peptides.

7.4 Detection of AQP4 antibody using bioelectronic sensor

The sensing ability of this sensor was evaluated using antibodies in PBS solution. A PBS droplet of 20 μl was added to the peptide-immobilized CNT channel, and the sample solution containing AQP4 antibody (ab46182, Abcam, UK) was injected. Figure 7.4(a) shows the real-time conductance of the sensor with concentrations of AQP4 antibody ranging from 1 ng/l to 1 μg/l. Each AQP4 extracellular loop peptide-based sensor showed a dose-dependent response. The sensor was able to detect AQP4 antibody at a concentration as low as 1 ng/l with AQP4 loop E. In our previous research for the detection of AQP4 antibody, nanovesicle-based CNT biosensor showed the detection limit of 10 ng/l antibody.[108] The LOD was improved by ten-fold due to the shortened distance between CNTs and antibody, since the small size peptides were used. Figure 7.4(b) shows the normalized sensitivity of each peptide to different concentrations of AQP4 antibody. AQP4 loop E showed the highest sensitivity to AQP4 antibody among the three peptides. This result was attributed to the different affinity of each peptide with the antibody and different lengths of the peptides on the CNT channel.

(a)

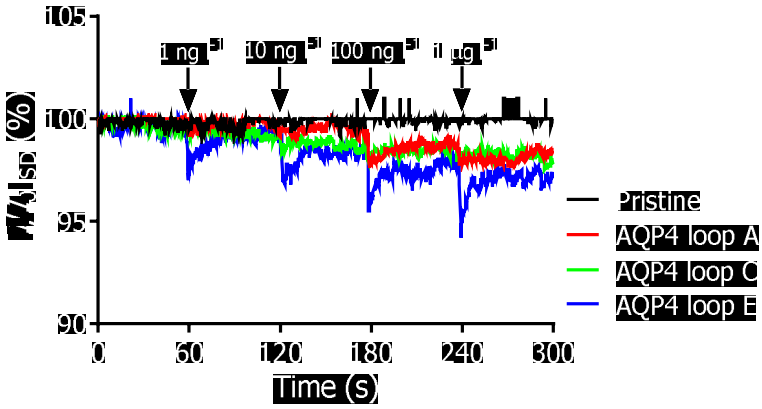

(b)

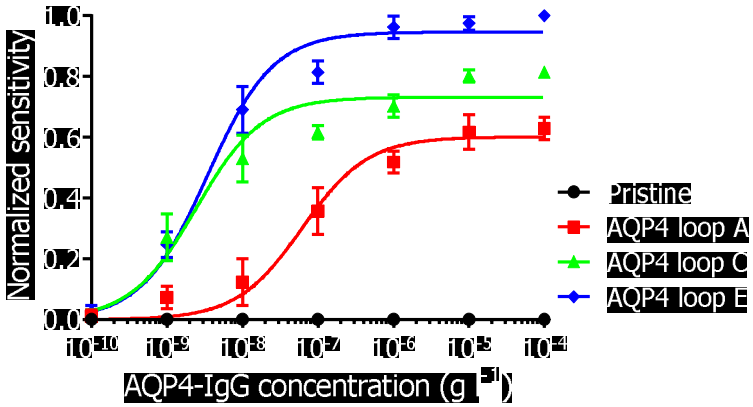

Figure 7.4 Detection of AQP4 antibody using peptide-based bioelectronic sensor. (a) Real-time responses of AQP4 loop peptide-based CNT-FETs to AQP4 antibody at concentrations ranging from 1 ng/l to 1 µg/l. (b) Normalized sensitivity of biosensors based on pristine CNTs (black line), CNTs functionalized with AQP4 loop A (red line), C (green line) and E (blue line) to antibody. Error bars, s. e. m. three replicates.

7.5 Detection of AQP4 antibody in human serum using bioelectronic sensor

It was reported that the antibody level of NMO patients is 13.984 ± 5.981 g/l.[163] To evaluate the usability of the sensor for the diagnosis of NMO, 1g/l of AQP4 antibody in human serum (H4522, SIGMA, US) was tested. Serum samples containing AQP4 antibody were prepared to $1:10^5$ dilution in PBS to avoid a non-specific response (Lim et al., 2014). As shown in Fig. 5a, the sensor did not respond to the human serum without AQP4 antibody, but the conductance decreased when antibodies were present in the serum samples. The RSD values were 8.33% with AQP4 loop A, 23.08% with AQP4 loop C and 2.17% with AQP4 loop E (n = 3) (Fig. 5b). These results indicate that the sensor can be effectively used for the rapid and easy diagnosis of NMO. This biosensor is for a single-use. It was difficult to recover the current signal after use, since the binding of antibody and peptide was not completely removed with washing process. However, mass production of CNT-based sensor is available with the lithography method and it requires only a small volume of peptide for the functionalization. It also has advantages in simple and fast detection of antibody without complex pretreatment procedures.

(a)

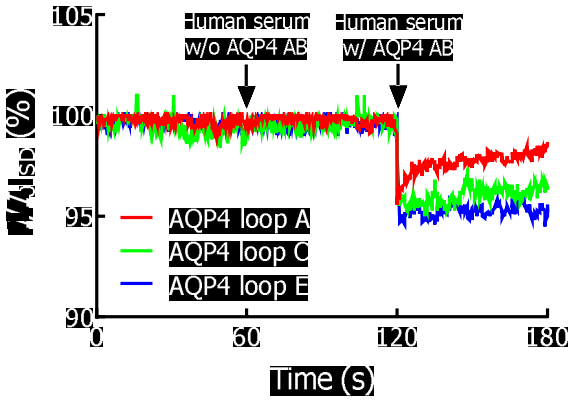

(b)

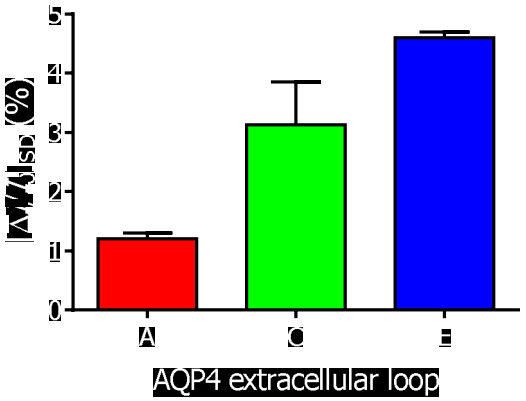

Figure 7.5 Detection of AQP4 antibody in human serum using peptide-based bioelectronic sensor. (a) Real-time response to 1 g/l of AQP4 antibody in $1/10^5$-diluted human serum. (b) Quantitative comparison of conductance change among AQP4 extracellular loop A (red line), C (green line) and E (blue line). Error bars, s. e. m. three replicates.

7.6 Conclusions

We developed a rapid sensor for the diagnosis of NMO using peptide-based CNT-FET. AQP4 extracellular loop peptides, which bind with the serum biomarker of NMO, were synthesized and three molecules of Phe were added to the C-terminal for immobilization on CNTs. The synthesized peptides were directly immobilized onto CNT channels in the FET sensor. The constructed biosensor showed p-type FET characteristics and could detect a positively charged antibody. The sensor can detect 1 ng/l of AQP4 antibody with the AQP4 loop E peptide. Moreover, human serum antibody was detected without any pretreatment. Due to its high sensitivity and rapidity, this biosensor can be effectively used as a simple and easy diagnostic method for NMO.

Chapter 8.

Overall discussion and further suggestions

Chapter 8. Overall discussion and further suggestions

Bioelectronic sensors that combine biomolecules and electronics have been developed for sensitive and selective analytical tools. Biomolecules, such as DNA, protein, and cells, were used as primary recognition elements. Carbon nanomaterials, such as carbon nanotubes, conducting polymers and graphene, were utilized for rapid signal amplifications. Various receptor-ligand bindings and their action potentials were compatible to convert into electrical signals. The bioelectronic sensors have advantages in cost efficiency, small size, fast response, high sensitivity and selectivity. It is expected that integrating various kinds of receptors with carbon nanomaterials could be applied to diverse areas in the human life.

In the thesis, CNT-based bioelectronic sensors using receptor proteins and peptides were developed and applied to environmental monitoring, disease diagnosis and food quality assessment.

In chapter 4, a bioelectronic sensor using human olfactory nanovesicle for detection of odor compounds in water pollution was presented. Artificial olfactory systems were constructed and hORs were screened as specific receptors for the detection of water contamination indicators. Olfactory nanovesicles were produced from the mammalian cells expressing the hORs. CNT-FETs were functionalized with the olfactory nanovesicles. The bioelectronic nose sensitively and selectively detected target molucules and the detection limit was 10 mg/l, a sufficiently low level for the assessment of water quality. The water contamination indicators were detected in various water samples without pre-treatment. These results offer the simple and rapid method for monitoring of water quality in real environments.

In chapter 5, a bioelectronic sensor using human olfactory nanovesicle for detection of VOCs from *in vitro* diabetic models was presented. *In vitro* models of diabetes were constructed by inducing insulin resistance in 3T3-L1 adipocytes and L6 skeletal muscle cells with a treatment of palmitic acid.

VOCs in the headspace of both cells were collected and analyzed using SPME-GC/MS. 17ODYA was selected as the potential biomarker for early diagnosis of diabetes. Human OR was screened for the selective recognition of 17ODYA and produced from the artificial olfactory cells as nanovesicles. The nanovesicle-based bioelectronic nose detected 10 fM of 17ODYA in dose-dependent manner with high selectivity. This approach can be used for efficient diagnosis of diseases that biomarkers are not known.

In chapter 6, a portable and multiplexed bioelectronic sensor using human olfactory and taste receptor proteins for assessment of food quality was presented. Olfactory and taste receptors were produced in *E. coli*, and immobilized onto a multi-channel CNT-FET. A miniaturized current measurement platform was combined with the multi-channel bioelectronic sensor and electrical signals against four different food contamination indicators were simultaneous detected. Various pattern recognitions of complex mixtures were successfully analyzed with the developed device. The bioelectronic device was suitable for monitoring of food freshness and is expected to be used as an on-site sensing platform.

In chapter 7, a peptide-based bioelectronic sensor using extracellular loops of aquaporin for diagnosis of NMO was presented. AQP4 extracellular loop peptides were synthesized with the addition of triple Phe in C-terminal and immobilized onto CNT channels. The peptide-based bioelectronic sensor detected 1 ng/l of NMO-IgG with AQP4 loop E peptide. Antibodies in human serums were detected without pretreatment. The bioelectronic sensor can be used for rapid and simple detection of disease biomarkers.

In this research, nanovesicles derived from receptor expressing cells, proteins produced in *E. coli* and peptides derived from receptors were utilized as primary recognition elements of the bioelectronic sensors. Nanoveislces were immobilized onto PDL-coated CNT-FET surface using charge-charge interactions, proteins were immobilized onto Ni-modified

CNT-FET using Ni-NTA interactions, and peptides were directly immobilized CNT channels using pi-pi interactions CNTs and the aromatic rings of Phe. In the nanovesicle-based bioelectronic sensors that mimic the human olfactory mechanism, odor and olfactory receptor binding triggered calcium influx in nanovesicles and influenced the current changes of the transistor. In the protein-based bioelectronic sensors, structural changes of charged amino acids in the receptor proteins influenced the current changes. In the peptide-based bioelectrocnic sensors, positively charged target molecules influence the field effect on the transistor.

For environmental monitoring, the water contamination indicators, GSM and MIB, were specifically recognized by hOR51S1 and hOR3A4. For food quality assessment, octanal (beef contamination indicator) was detected with OR2J2 and OR2W1, hexanal (lipid oxidation indicator) was detected with OR2W1, TMA (seafood decomposition indicator) was detected with TAAR5, and goitrin were detected with TAS2R38. For the disease diagnosis, 17ODYA, VOC in the diabetes *in vitro* model, was detected with hOR51A4, and NMO serum biomarker was detected with AQP4 extracellular loop-derived peptide. Using athe combination of novel receptors and nanomaterial-based transistor, bioelectronic sensors are expected to be applied in various new area.

For the practical application of bioelectronic sensors, the miniaturized current measurement was customized with the receptor-functionalized CNT-FET sensor. The combined bioelectronic device was operated with laptop computer and the portability of the bioelectronic sensor was promoted. Multiplexed bioelectronic sensor enabled the simultaneous detection of different target molecules and pattern recognitions of target molecules were available. These techniques can improve the accuracy of the detected sensor signals.

Reusability of the bioelectronic sensors is also important for their practical applications. Protein- and peptide-based bioelectronic sensors are

relatively stable than nanovesicle-based bioelectronics sensors and can be used again after washing steps. However, nanovesicle-based bioelectronic sensors, which utilized calcium ion influx as signal measurement principles, cannot be reused. When calcium ions inside nanovsicles are saturated, the nanovesicle-based sensors cannot discharge calcium ions. Recently, an ion-channel-coupled receptor-based platform was developed for the measurement of GPCR activities.[164] This platform uses GPCR fused with a Kir 6.2 channel and potassium ion influx as current change principles. With the integration of outward-rectifying potassium channels such as blue light-induced and voltage-gated potassium channels.[165,167] The nanovesicle-based bioelectronic sensors are expected to be reused with the controlled influx and outflux of potassium ions.

Moreover, we compared bioelectronic sensor using receptor proteins with traditional methods. When freshness of oyster samples was analyzed with the bioelectronic sensor, human sensory evaluation and GC/MS, the bioelectronic sensor has positive correlation with other analytical methods. The signal observed with the bioelectronic sensor was two days faster than other methods. These results offer the rapid and simple tool for early detection food contamination. It is also expected that the sensitive bioelectronic sensor using disease-related receptor proteins can be developed for novel diagnostic tools which have difficulty in early-phase detection. Bioelectronic sensors that have the selectivity of the nature system and the sensitivity of nanoelectronics can be used for the study of unknown phenomena of the currently existing experimental methods. The combinatorial developments of bioelectronic sensors and biogenerators could be applied to not only biological signal detections but also reproduction of biological signals based on the recognized patterns.

Bibliography

1. Willner, I. and Willner, B., Biomaterials integrated with electronic elements: en route to bioelectronics, ***Trends Biotechnol.*** 19, 222-230 (2001)
2. Ingebrandt, S., Bioelectronics: Sensing beyond the limit, ***Nat. Nanotechnol.*** 10, 734-735 (2015)
3. Katz, E. and Willner, I., Biomolecule-functionalized carbon nanotubes: applications in nanobioelectronics, ***ChemPhysChem*** 5, 1084-1104 (2004)
4. Noy, A., Bionanoelectronics, ***Adv. Mater.*** 23, 807-820 (2011)
5. Zhang, A. and Lieber, C. M., Nano-Bioelectronics, ***Chem. Rev.*** 116, 215-257 (2016)
6. Pierce, K. L., Premont, R. T. and Lefkowitz, R. J., Seven-transmambrane receptors, ***Nat. Rev. Mol. Cell Biol.*** 3, 639-650 (2002)
7. Zhang, R. and Xie, X., Tools for GPCR drug discovery, ***Acta Pharmacol. Sin***. 33, 372-384 (2012)
8. Zhuang, H. and Matsunami, H., Evaluating cell-surface expression and measuring activation of mammalian odorant receptors in heterologous cells, ***Nat. Protoc.*** 3, 1402-1413 (2008)
9. Pick, H., Schmid, E. L., Tairi, A. P., Ilegems, E., Hovius, R. and Votel, H., Investigating cellular signaling reactions in single attoliter vesicles, ***J. Am. Chem. Soc.*** 127, 2908-2912 (2005)
10. Lee, M., Im, J., Lee, B. Y., Myung, S., Huang, L., Kwon, Y. K. and Hong, S., Linker-free directed assembly of high-

performance integrated devices based on nanotubes and nanowires, ***Nat. Nanotechnol.*** 1, 66-71 (2006)

11. Wu, T. Z., Lo, Y. R. and Chan, E. C., Exploring the recognized bio-mimicry materials for gas sensing, ***Biosens. Bioelectron.*** 16, 945-953 (2001)
12. Chen, R. J., Zhang, Y., Wang, D. and Dai, H., Noncovalent sidewall functionalization of single-walled carbon nanotubes for protein immobilization, ***J. Am. Chem. Soc.*** 123, 3838-3839 (2001)
13. Poenitzsch, V. Z., Winters, D. C., Xie, H., Dieckmann, G. R., Dalton, A. B. and Musselman, I. H., Effect of electron-donating and electron-withdrawing groups on peptide/single-walled carbon nanotube interactions, ***J. Am. Chem. Soc.*** 129, 14724-14732 (2007)
14. Klabunde, T. and Hessler, G., Drug-design strategies for targeting G-protein-coupled receptors, ***ChemBioChem*** 3, 928-944 (2002)
15. Miyano, K., Sudo, Y., Yokoyama, A., Hisaoka-Nakashima, K., Morioka, N., Takebayashi, M., Nakata, Y., Higami, Y. and Uezono, Y., History of the G protein-couppled receptor (GPCR) assays from traditional to a state-of-the-art biosensor assay, ***J. Pharmacol. Sci*** 126, 302-309 (2014)
16. Thomse, W., Frazer, J, and Unett, D., Functional assays for screening GPCR targets, ***Curr. Opin. Biotechnol.*** 16, 655-665 (2005)
17. Wang, J., Nanomaterial-based amplified transduction of biomolecular interactions, ***Small*** 1, 1036-1043 (2005)
18. Wang, J., Nanomaterial-based electrochemical biosensors, ***Analyst*** 130, 421-426 (2005)

19. Yang, W., Ratinac, K. R., Ringer, S. P., Thordarson, P., Gooding, J. J. and Braet, F., Carbon nanomaterials in biosensors: should you use nanotubes or graphene?, ***Angew. Chem. Int. Ed. Engl.*** 49, 2114-2138 (2010)
20. Liu, S. and Guo, X., Carbon nanomaterials field-effect-transistor-based biosensors, ***NPG Asia Materials*** 4, e23 (2012)
21. Kim, T. H., Lee, S. H., Lee, J., Song, H. S., Oh, E. H., Park, T. H. and Hong, S., Single-carbon-atomic-resolution detection of odorant molecules using a human olfactory receptor-based bioelectronic nose, ***Adv. Mater.*** 21, 91-94 (2009)
22. Lee, S. H. and Park, T. H., Recent advances in the development of bioelectronic nose, ***Biotechnol. Bioprocess Eng.*** 15, 22-29 (2010)
23. Lee, S. H., Jin, H. J., Song, H. S., Hong, S. and Park, T. H., Bioelectronic nose with high sensitivity and selectivity using chemically functionalized carbon nanotube combined with human olfactory receptor, ***J. Biotechnol.*** 157, 467-472 (2012)
24. Jin, H. J., Lee, S. H., Kim, T. H., Park, J., Song, H. S., Park, T. H. and Hong, S., Nanovesicle-based bioelectronic nose platform mimicking human olfactory signal transduction, ***Biosens. Bioelectron.*** 35, 335-341 (2012)
25. Song, H. S., Jin, H. J., Ahn, S. R., Kim, D., Lee, S. H., Kim, U. K., Simons, C. T., Hong, S. and Park, T. H., Bioelectronic tongue using heterodimeric human taste receptor for the discrimination of sweetners with human-like performance, ***ACS Nano*** 8, 9781-9789 (2014)
26. Kim, B., Song, H. S., Jin, H. J., Park, E. J., Lee, S. H., Lee, B. Y., Park, T. H. and Hong, S., Highly-selective and sensitive detection of neurotransmitters using receptor-modified single-

walled carbon nanotube sensors, ***Nanotechnology*** 24, 285501 (2013)

27. Nel, A. E., Madler, L., Velegol, D., Xia, T., Hoek, E. M., Somasundaran, P., Klaessig, F., Castranova, V. and Thompson, M., Understanding biophysicochemical interactions at the nano-bio interface, ***Nat. Mater.*** 8, 543-557 (2009)
28. McCammon, J. A., Theory of biomolecular recognition, ***Curr. Opin. Struct. Biol.*** 8, 245-249 (1998)
29. Avouris, P., Chen, Z. and Perebeinos, V., Carbon-based electronics, ***Nat. Nanotechnol.*** 2, 605-615 (2007)
30. Yang, N., Chen, X., Ren, T., Zhang, P. and Yang, D., Carbon nanotube based biosensors, ***Sens. Actuators B Chem.*** 207, 690-715 (2015)
31. Kuila, T., Bose, S., Khanra, P., Mishra, A. K., Kim, N. H. and Lee, J. H., Recent advances in graphene-based biosensors, ***Biosens. Bioelectron.*** 26, 4637-4648 (2011)
32. Schoning, M. J. and Poghossian, A., Recent advances in biologically sensitive and field-effect transistors (BioFETs), ***Analyst*** 127, 1137-1151 (2002)
33. Matsumoto, A. and Miyahara, Y., Current and emerging challenges of field effect transistor based bio-sensing, ***Nanoscale*** 5, 10702-10718 (2013)
34. Baneres, J. L., Popot, J. L. and Mouillac, B., New advances in production and functional folding of G-protein-coupled receptors, ***Trends Biotechnol.*** 29, 314-322 (2011)
35. Benson, D. E., Conrad, D. W., de Lorimier, R. M., Trammell, S. A. and Hellinga, H. W., ***Science*** 293, 1641-1644 (2001)

36. Willner, I., Willner, B. and Katz, E., Functional biosensor systems via surface-nanoengineering of electronic elements, ***J. Biotechnol.*** 82, 325-355 (2002)
37. Braslavsky, I., Hebert, B., Kartalov, E. and Quake, S. R., Sequence information can be obtained from single DNA molecules, ***Proc. Natl. Acad. Sci. U. S. A.*** 100, 3960-3964 (2003)
38. International Human Genome Sequencing Consortium, Finishing the euchromatic sequence of the human genome, ***Nature*** 431, 931-945 (2004)
39. Keren, K., Berman, R. S., Buchstab, E., Sivan, U. and Braun E., DNA-templated carbon nanotube field-effect transistor, ***Science*** 302, 1380-1382 (2003)
40. Napier, M. E., Loomis, C. R., Sistare, M. F., Kim, J., Eckhardt, A. E. and Thorp, H. H., Probing biomolecule recognition with electron transfer: electrochemical sensors for DNA hybridization, ***Biochonjug. Chem.*** 8, 906-913 (1997)
41. Sakata, T. and Miyahara, Y., DNA senquencing based on intrinsic molecular charges, ***Angew. Chem. Int. Ed. Engl.*** 45, 2225-2228 (2006)
42. Sakata, T. and Miyahara, Y., Potentiometric detection of single nucleotide polymorphism by using a genetic field-effect transistor, ***Chembiochem*** 6, 703-710 (2005)
43. Staii, C., Jornson, A. T. Jr., Chem, M. and Gelrepin, A., DNA-decorated carbon nanotubes for chemical sensing, ***Nano Lett.*** 5, 1774-1778 (2005)
44. So, H. H., Won, K., Kim, Y. H., Kim, B. K., Ryu, B. H., Na, P. S., Kim, H. and Lee, J. O., Single-walled carbon nanotube biosensors using aptamers as molecular recognition elements, ***J. Am. Chem. Soc.*** 127, 11906-11907 (2005)

45. de la Rica, R. and Matsui, H., Applications of peptide and protein-based materials in biotechnology, ***Chem. Soc. Rev.*** 39, 3499-3509 (2010)
46. Yin, L. T., Chou, J. C., Chung, W. Y., Sun, T. P., Hsiung, K. P. and Hsiung, S. K., Glucose ENFET doped with MnO 2 powde, ***Sens. Actuators B Chem.*** 76, 187-192 (2001)
47. Willner, I. I. and Katz, E., Integration of layered redox proteins and conductive supports for bioelectronic applications, ***Angew. Chem. Int. Ed. Engl.*** 38, 1180-1218 (2000)
48. Zheng, G., Patolsky, F., Cui, Y., Wang, W. U. and Lieber, C. M., Multiplexed electrical detection of cancer markers with nanowire sensor arrays, ***Nat. Biotechnol.*** 23, 1294-1301 (2005)
49. Du, L., Wu, C., Liu, Q., Huang, L. and Wang, P., Recent advances in olfactory receptor-based biosensors, ***Biosens. Bioelectron.*** 42, 570-580 (2013)
50. Ceto, X., Voelcker, N. H. and Prieto-Simon, B., Bioelectronic tongues: New trends and applications in water and food analysis, ***Biosens. Bioelectron.*** 79, 608-626 (2016)
51. Venkatakrishnan, A. J., Deupi, X., Lebon, G., Tate, C. G., Schertler, G. F. and Babu, M. M., Molecular signatures of G-protein-coupled receptors, ***Nature*** 494, 185-193 (2013)
52. Gelis, L., Wolf, S., Hatt, H., Neuhaus, E. M. and Gerwert, K., Prediction of a ligand-binding niche within a human olfactory receptor by combining site-directed mutagenesis with dynamic homology modeling, ***Angew. Chem. Int. Ed. Engl.*** 51, 1274-1278 (2012)
53. Duan, X., Gao, R., Xie, P., Cohen-Karni, T., Choe, H. S., Tian, B., Jiang, X. and Lieber, C. M., Intracellular recording

of action potentials by an extracellular nanoscale field-effect transistor, ***Nat. Nanotechnol.*** 7, 174-179 (2011)

54. Nirsch, C., Roesslein, M., Krung, H. F. and Wick, P., Nanomaterial cell interactions: are current in vitro tests reliable?, ***Nanomedicine*** 6, 837-847 (2011)
55. Patolsky, F., Timko, B. P., Fang, Y., Greytak, A. B., Zheng, G. and Lieber, C. M., Detection, stimulation, and inhibition of neuronal signals with high-density nanowire transistor arrays, ***Science*** 313, 1100-1104 (2006)
56. Wang, C. W., Pan, C. Y., Wu, H. C., Shih, P. Y., Tsai, C. C., Liao, K. T., Lu, L. L., Hsieh, W. H., Chen, C. D. and Chen, Y. T., In situ detection of chromogranin a released from living neurons with a single-walled carbon-nanotube field-effect transistor, ***Small*** 3, 1350-1355 (2007)
57. Ta, V. T., Park, J., Park, E. J. and Hong, S., Reusable floaring-electrode sensor for the quantitative electrophisiological monitoring of a nonadherent cell, ***ACS Nano*** 8, 2206-2213 (2014)
58. Dumitrescu, I., Unwin, P. R. and Macpherson, J. V., Electrochemistry at carbon nanotubes: perspective and issues, ***Chem. Commun.*** 45, 6886-6901 (2009)
59. Lee, M., Im, J., Lee, B. Y., Myung, S., Kang, J., Huang, L., Kown, Y. K. and Hong, S., Linker-free directed assembly of high-performance integrated devices based on nanotubes and nanowires, ***Nat. Nanotechnol.*** 1, 66-71 (2006)
60. Banerjee, S., Hemraj-Benny, T. and Wong, S. S, Covalent surface chemistry of single-walled carbon nanotubes, ***Adv. Mater.*** 17, 17-29 (2005)

61. Zhao, Y. L. and Stoddart, J. F., Noncovalent functionalization of single-walled carbon nanotubes, ***Acc. Chem. Res.*** 42, 1161-1171 (2009)
62. Xia, L., Wei, Z. and Wan, M., Conducting polymer nanostructures and their application in biosensors, ***J. Colloid Interface Sci.*** 341, 1-11 (2010)
63. An, K. H., Jeong, S. Y., Hwang, H. R. and Lee, Y. H., Enhanced sensitivity of a gas sensor incorporating single-walled carbon nanotube-polypyrrole nanocomposites, ***Adv. Mater.*** 16, 1005-1009 (2004)
64. Gerard, M., Chaubey, A. and Malhotra, B. D., Applications of conducting polymers to biosensors, ***Biosens. Bioelectron.*** 17, 345-359 (2002)
65. Ramanathan, K., Mehrotra, R., Jayaram, B., Mrythy, A. S. N. and Malhotra, B. D., Simulation of electrochemical process for glucose oxidase immobilized conducting polymer, ***Anal. Lett.*** 29, 1477-1484 (1996)
66. Gambhir, A., Gerard, M., Mulchandani, A. K. and Malhotra, B. D., Coimmobilization of urease and glutamate dehydrohenase in electrochemically prepared polypyrrole-polyvinyl sulfonate films, ***Appl. Biochem. Biotechnol.*** 96, 249-257 (2001)
67. Chaubey, A., Gerard, M., Singhai, R., Singh, A. S. and Malhotra, B. D., Immobilization of lactate dehydrogenase on electrochemically prepared polypyrrole-polyvinyl sulphonate composite films for application to lactate biosensors, ***Electrochim. Acta*** 46, 723-729 (2000)
68. Ramanathan, K., Pandey, S. S., Kumar, R., Gulati, A., Murthy, A. S. N. and Malhotra, B. D., Covalent immobilization of

glucose oxidase to poly(o-amino benzoic acid) for application to glucose biosensor, ***J. Appl. Polym. Sci.*** 78, 662-667 (2000)

69. Zhao, Y., Liu, B., Pan, L. and Yu, G., 3D nanostructured conductive polymer hydrogels for high-perforance electrochamical devices, ***Energy Environ. Sci.*** 6, 2856-2870 (2013)
70. Li, L., Shi, Y., Pan, L. and Yu, G., Rational design and applications of conducting polymer hydrogels as electrochemical biosensors, ***J. Mater. Chem. B*** 3, 2920-2930 (2015)
71. Shao, Y., Wang, J., Wu, H., Liu, J., Aksay, I. A. and Liu, Y., Graphene based electrochemical sensors and biosensors: a review, ***Electroanalysis*** 22, 1027-1036 (2010)
72. Noveselov, K. S., Geim, A. K., Morozov, S. V., Jiang, D., Zhang, Y., Dubonos, S. V., Grigorieva, I. V. and Firsov, A. A., Electric field effect in atomically thin carbon films, ***Science*** 306, 666-669 (2004)
73. Reina, A., Jia, X., Ho, J., Nezich, D., Son, H., Bulovic, V., Dresselhaus, M. S. and Kong, J., Large area, few-layer graphene films on arbitary substrates by chemical vapor deposition, ***Nano Lett.*** 9, 30-35 (2009)
74. Pinto, A. M., Goncalves, I. C. and Magalhaes, F. D., Graphene-based materials biocompatibility: a review, ***Colloids Surf. B Biointerfaces*** 111, 188-202 (2013)
75. Sun, X., Sun, H., Li, H. and Peng, H., Developing polymer composite materials: carbon nanotbes of graphene?, ***Adv. Mater.*** 25, 5153-5376 (2013)
76. El-Kady, M. F., Strong, V., Dubin, S. and Kaner, R. B., Laser acribing of high-performance and flexible graphene-based electrochemical capacitors, ***Science*** 335, 1326-1330 (2012)

77. Oh, E. H., Song, H. S. and Park, T. H., Recent advances in electronic and bioelectronic noses and their biomedical applications, ***Enzyme Microb. Technol.*** 48, 427-437 (2011)
78. Buck, L. and Axel, R., A novel multigene family may encode odorant receptors: a molecular basis for odor recognition, ***Cell*** 65, 175-187 (1991)
79. Jiang, Y. and Matsunami, H., Mammalian odorant receptors: functional evolution and variation, ***Curr. Opin. Neurobiol.*** 34, 54-60 (2015)
80. Axel, R., Scents and sensibility: a molecular logic of olfactory perception, ***Angew. Chem. Int. Ed. Engl.*** 44, 6110-6127 (2005)
81. Malnic, B., Hirono, J., Sato, T. and Buck, L. B., Combinatorial receptor codes for odors, ***Cell*** 96, 713-723 (1999)
82. Hallem, E. A. and Carlson, J. R., Coding of odors by a receptor repertoire. ***Cell*** 125, 143-160 (2006)
83. Bushddid, C., Magnasco, M. O., Vosshall, L. B. and Keller, A., Humans can discriminate more than 1 trillion olfactory stimuli, ***Science***. 343, 1370-1372 (2014)
84. Kim, T. H., Lee, S. H., Lee, J., Song, H. S., Oh, E. H., Park, T. H. and Hong, S., Single-carbon-atomic resolution detection of odorant molecules using a human olfactory receptor-based bioelectronic nose, ***Adv. Mater.*** 21, 91-94 (2009)
85. Kauffman, D. R. and Star, A.,Electronically monitoring biological interactions with carbon nanotube field-effect transistors, ***Chem. Soc. Rev.*** 37, 1197-1206 (2008)
86. Lee, S. H, Kwon, O. S., Song, H. S., Park, S. J., Sung, J. H., Jang, J. and Park, T. H., Mimicking the human smell sensing

mechanism with an artificial nose platform, ***Biomaterials*** 33, 1722-1729 (2012)

87. Park, S. J., Kwon, O. S., Lee, S. H., Song, H. S., Park, T. H. and Jang, J., Ultrasensitive flexible graphene based field-effect transistor (FET)-type bioelectronic nose, ***Nano Lett.*** 12, 5082-5090 (2012)

88. Yoon, H., Lee, S. H., Kown, O. S., Song, H. S. Oh, E. H., Park, T. H. and Jang, J., Polypyrrole nanotubes conjugated with human olfactory receptors: high-performance transducers for FET-type bioelectronic noses, ***Angew. Chem. Int. Ed. Engl.*** 48, 2755-2758 (2009)

89. Lim, J. H., Park, J., Oh, E. H., Ko, H. J., Hong, S. and Park, T. H., Nanovesicle-based bioelectronic nose for the diagnosis of lung cancer from human blood, ***Adv. Healthc. Mater.*** 3, 360-366 (2014)

90. Son, M., Cho, D. G., Lim, J. H., Park, J., Hong, S., Ko, H. J. and Park, T. H., Real-time monitoring of geosmin and 2-methylisoborneol, represenrative odor compounds in water pollution using bioelectronic nose with human-like performance, ***Biosens. Bioelectron.*** 74, 199-206 (2015)

91. Park, J., Lim, J. H., Jin, H. J., Namgung, S., Lee, S. H., Park, T. H. and Hong, S., A bioelectronic sensor based on canine olfactory nanovesicle-carbon nanotube hybrid structures for the fast assessment of food quality, ***Analyst*** 137, 3249-3254 (2012)

92. Lim, J. H., Park, J., Ahn, J. H., Hong, S. and Park, T. H., A peptide receptor-based bioelectronic nose for the real-time determination of seafood quality, ***Biosens. Bioelectron.*** 39, 244-249 (2013)

93. Lee, S. H., Lim, J. H., Park, J., Hong, S. and Park, T. H., Bioelectronic nose combined with a microfluidic system for the detection of gaseous trymethylamine, ***Biosens. Bioelectron.*** 71, 179-185 (2015)
94. Ahn, J. H., Lim, J. H., Park, J., Oh, E. H., Son, M., Hong, S. and Park, T. H., Screening of target-specific olfactory receptor and development of olfactory biosensor for the assessment of fungal contamination in grain, ***Sens. Actuators. B Chem.*** 210, 9-16 (2015)
95. Kwon, O. S., Song, H. S., Park, S. J., Lee, S. H., An, J. H., Park, J. W., Yanh, H., Bae, J., Park, T. H., Jang, J., An ultrasensitive, selective, multiplexed superbioelectronic nose that mimics the human sense of smell, ***Nano Lett.*** 15, 6559-6567 (2015)
96. Nara, K., Saraiva, L. R., Ye, X. and Buck, L. B., A large-scale analysis of odor coding in the olfactory epithelium, ***J. Neurosci.*** 31, 9179-9191 (2011)
97. Chandrashekar, J., Hoon, M. A., Ryba, N. J. P. and Zuker, C. S., The receptors and cells for mammalian taste, ***Nature*** 444, 288-294 (2006)
98. Smith, D. V. and St John, S. J., Neural coding of gustatory information, ***Curr. Opin. Neurobiol.*** 9, 427-435 (1999)
99. Smith, D. V., John, S. J. and Boughter, J. D., Neuronal cell types taste quality coding, ***Physiol. Behav.*** 69, 77-85 (2000)
100. Nelson, G., Chandrashekar, J., Hoon, M. A., Feng, L., Zhao, G., Ryba, N. J. P. and Zuker, C. S., An aminno-acid taste receptor, ***Nature*** 416, 199-202 (2002)
101. Nelson, G., Hoon, M. A., Chandrashekar, J., Zhang, Y., Ryba, N. J. and Zuker, C. S., Mammalian sweet taste receptors, ***Cell*** 106, 381-390 (2001)

102. Adler, E., Hoon, M. A., Mueller, K. L., Chandrashekar, J., Ryba, N. J. and Zuker, C. S., A novel family of mammalian taste receptors, ***Cell*** 100, 693-702 (2000)
103. Matsunami, H., Montmayeur, J. P. and Buck, L. B., A family of candidate taste receptors in human and mouse, ***Nature*** 404, 601-604 (2000)
104. Kim, T. H., Song, H. S., Jin, H. J., Lee, S. H., Namgung, S., Kim, U., Park, T. H. and Hong, S., "Bioelectronic super-taster" device based on taste receptor-cargon nanotube hybrid structures, ***Lab Chip*** 11, 2262-2267 (2011)
105. Song, H. S., Kwon, O. S., Lee, S. H., Park, S. J., Kim, U., Jang, J. and Park, T. H., Human taste receptor-functionalized field effect transistor as a human-like nanobioelectronic tongue, ***Nano Lett.*** 13, 172-178 (2013)
106. Lee, M., Jung, J. W., Kim, D., Ahn, Y. J., Hong, S. and Kwon, H. W., Discrimination of umami tastants using floating electrode-based bioelectronic tongue mimicking insect taste systems, ***ACS Nano*** 9, 11728-11736 (2015)
107. Jin, H. J., An, J. M., Park, J., Moon, S. J. and Hong, S., "Chemical-pain sensor" based on nanovesicle-carbon nanotube hybrid structures, ***Biosens. Bioelecton.*** 49, 86-91 (2013)
108. Park, E. J., Park, J., Song, H. S., Kim, S. J., Jung, K. C., Kim, S., Cho, D., Kim, D., Park, K. S. and Hong, S., Nanovesicle-based platform for the electrophysiological monitoring of aquaporin-4 and the real-time detection of its antibody, ***Biosens. Bioelectron.*** 61, 140-146 (2014)
109. Park, S. J., Song, H. S., Kwon, O. S., Chung, J. H., Lee, S. H., An, J. H., Lee, J. E., Yoon, H., Park, T. H. and Jang, J., Human dopamine receptor nanovesicles for gate-potential

modulators in high-performance field-effect transistor biosensors, ***Sci. Rep.*** 4, 4342 (2014)

110. Kwon, O. S., Ahn, S. R., Park, S. J., Song, H. S., Lee, S. H., Lee, J. S., Hong J. Y., Lee, J. S., You, S. A., Yoon, H., Park, T. H. and Jang, J., Ultrasensitive and selective recognition of peptide hormone using close-packed arrays of hPTHR-conjugated polymer nanoparticles, ***ACS Nano*** 6, 5549-5558 (2012)
111. Zaitlin, B. and Watson, S. B., Actinomycetes in relation to taste and odour in drinking water: Myths, tenets and truths, ***Water Res.*** 40, 1741-1753 (2006)
112. Parinet, J., Rodriguez, M. J. and Serodes, J., Influence of water quality on the presence of off-flavour compounds (geosmin and 2-methylisoborneol), ***Water Res.*** 44, 5847-5856 (2010)
113. Li, Z., Hobson, P., An, W., Burch, M. D., House, J. and Yang, M., Earthy odor compounds productions and loss in three cyanobacterial cultures, ***Water Res.*** 46, 5165-5173 (2012)
114. Polak, E. H. and Provasi, J., Odor sensitivity to geosmin enantiomers, ***Chem. Senses*** 17, 23-26 (1992)
115. Freeman, K. S., Harmful algal blooms. Musty warnings of toxicity, ***Environ. Health Perspect.*** 118, A473 (2010)
116. Lloyd, S. W., Lea, J. M., Zimba, P. V. and Grimm, C. C., Rapid analysis of geosmin and 2-methylisoborneol in water using solid phase micro extraction procedures, ***Water Res.*** 32, 2140-2146 (1998)
117. Watson, S. B., Brownlee, B., Satchwill, T. and Hargesheimer, E. E., Quantitative analysis of trace levels of geosmin and MIB in source and drinking water using headspace SPME, ***Water Res.*** 34, 2818-2828 (2000)

118. Goldsmith, B. R., Mitala, J. J., Josue, J., Castro, A., Lerner, M. B., Bayburst, T. H., Khamis, S. M., Jones, R. A., Brand, J. G., Sligar, S. G., Luetje, C. W., Gelperin, A., Rhodes, P. A., Discher, B. M. and Johnson, A. T., Biomimetic chemical sensors using nanoelectronic readout of olfactory receptor proteins, ***ACS Nano.*** 5, 5408-5416 (2011)

119. Zou, D. J., Chesler, A. and Firestein, S., How the olfactory bulb got its glomeruli: a just so story?, ***Nat. Rev. Neurosci.*** 10, 611-618 (2009)

120. Ko, H. J. and Park, T. H., Dual signal transduction mediated by a single type of olfactory receptor expressed in a heterologous system, ***Biol. Chem.*** 387, 59-68 (2006)

121. Wetzel, C. H., Oles, M., Wellerdieck, C., Kuczkowiak, M., Gisselmann, G. and Hatt, H., Specificity and sensitivity of a human olfactory receptor functionally expressed in human embryonic kidney 293 cells and Xenopus Laevis oocytes, ***J. Neurosci.*** 19, 7426-7433 (1999)

122. Goff, D. C. Jr., Gerstein, H. C., Ginsberg, H. N., Crushman, W. C., Margolis, K. L., Byington, R. P., Buse, J. B., Genuth, S., Probstfield, J. L. and Simons-Morton, D. G., Prevention of cardiovascular disease in persons with type 2 diabetes mellitus: current knowledge and rationale for the Action to Control Cardiovascular Risk in Diabetes (ACCORD) trial, ***Am. J. Cardiol.*** 99, 4i-20i (2007)

123. Phillips, M., Gleeson, K., Hughes, J. M., Greenberg, J., Cataneo, R. N., Baker, L. and McVay, W. P., Volatile organic compounds in breath as markers of lung cancer: a cross-sectional study, ***Lancet*** 353, 1930-1933 (1999)

124. Phillips, M., Cataneo, R. N., Ditkoff, B. A., Greenberg, J., Gunawardena, R., Kwon, C. S., Rahbari-Oskoui, F. and Wong, C., ***Breast J.*** 9, 184-191 (2003)

125. Altomare, D. F., Di Lena, M., Porcelli, F., Trizio, L., Travaglio, E., Tutino, M., Dragonieri, S., Memeo, V. and de Gennaro, G., Exhaled volatile organic compounds identify patients with colorectal cancer, ***Br. J. Surg.*** 100, 144-150 (2013)

126. Bays, H., Mandarino, L. and DeFronzo, R. A., Role of the adipocyte, free farry acids and ectopic fat in pathogenesis of type 2 diabetes mellitus: peroxisomal proliferator-activated receptor agonists provide a rational therapeutic approach, ***J. Clin. Endocrinol. Metab.*** 89, 463-478 (2004)

127. Schenk, S., Saberi, M. and Olefsky, J. M., Insulin sensitivity: modulation by nutrients and inflammation, ***J. Clin. Invest.*** 118, 2992-3002, (2008)

128. Nguyen, M. T., Satoh, H., Favelyukis, S., Babendure, J. L., Imamura, T., Sbodio, J. I., Zalevsky, J., Dahiyat, B. I., Chi, N. W. and Olefsky, J. M., JNK tumor necrosis factor-alpha mediate free fatty acid-induced insulin resistance in 3T3-L1 adipocytes, ***J. Biol. Chem.*** 280, 35361-35371 (2005)

129. Boden, G., Fatty acid-induced inflammation and insulin resistance in skeletal muscle and liver, ***Curr. Diab. Rep.*** 6, 177-181 (2006)

130. Glatz, R. and Bailey-Hill, K., Mimicking nature's noses: from receptor deorphaning to olfactory biosensing, ***Prog. Neurobiol.*** 93, 270-296 (2011)

131. Stitzel, S. E., Aernecke, M. J. and Walt, D. R., Artificial noses, ***Annu. Rev. Biomed. Eng.*** 13, 1-25 (2011)

132. Firestein, S., How the olfactory system makes sense of scents, ***Nature*** 413, 211-218 (2001)
133. Zou, Z. and Buck, L. B., Combinatorial effects of odorant mixes in olfactory cortex, ***Science*** 311, 1477-1481 (2006)
134. Yang, H., Song, H. S., Ahn, S. R. and Park, T. H., Purification and functional reconstitution of human olfactory receptor expressed in Escherichia coli, ***Biotechnol. Bioproc. E.*** 20, 423-430 (2015)
135. Saito, H., Chi, Q. Zhuang, H. Matsunami, H. and Mainland, J. D., Odor coding by a mammalian receptor repertoire, ***Sci. Signal.*** 2, ra9 (2009)
136. Wallrabenstein, I., Kuklan, J., Weber, L., Zborala, S., Werner, M., Altmuller, J., Becker, C., Schmidt, A., Hatt, H., Hummel, T. and Gisselmann, G, Human trace amine-associated receptor TAAR5 can be activated by trimethylamine, ***PLOS One*** 8, e54950 (2013)
137. Wooding, S., Gunn, H., Ramos, P., Thalmann, S., Xing, C. and Meyerhof, W., Genetics and bitter taste responses to goitrin, a plant toxin found in vegetables, ***Chem. Senses*** 35, 685-692 (2010)
138. Tait, E., Perry, J. D., Stanforth, S. P. and Dean, J. R., Identification of volatile organic compounds produced by bacteria using HS-SPME-GC-MS, ***J. Chromatogr. Sci.*** 52, 363-373 (2014)
139. Marsili, R. T., Comparison of Solid-phase microextraction and dynamic headspace methods for the gas chromatographic-mass spectrometric analysis of light-induced lipid oxidation products in milk, ***J. Chromatogr. Sci.*** 37, 17-23 (1999)
140. Hedegaard, R. V., Kristensen, D., Nielsen, J. H., Frost, M. B., Ostdal, H., Hermansen, J. E., Kroger-Ohlsen, M. and Skibsted,

L. H., Comparison of descriptive sensory analysis and chemical analysis for oxidative changes in milk. ***J. Diary Sci.*** 89, 495-504 (2006)

141. Dalgaard, P., Madsen, H. L., Samieian, N. and Emborg, J., Biogenic amine formation and microbial spoilage in chilled garfish (belone belone belone) – effect of modified atmosphere packaging and previous frozen storage, ***J. Appl. Microbiol.*** 101, 80-95 (2006)
142. Kiefer, H., Kriefer, J., Olszewski, J. D., Von Heijne, G., Prestwich, G. D. and Breer, H., Expression of an olfactory receptor in Escherichia coli: purification, reconstitution, and ligand binding, ***Biochemistry*** 35, 16077-16084 (1996)
143. Kaiser, L., Graveland-Bikker, J., Steuerwald, D., Vanberghem, M., Herlihy, K. and Zhang, S, Efficient cell-free production of olfactory receptors: detergent optimization, structure, and ligand binding analyses, ***Proc. Natl. Acad. Sci. U. S. A.*** 2008, 105, 15726-15731 (2008)
144. Vivian, J. T. and Callis, P. R., Mechanisms of tryptophan fluorescence shifts in proteins. ***Biophys. J.*** 80, 2093-2109 (2001)
145. Graff, R. A., Swanson, T. M. and Strano, M. S., Synthesis of nickel-nitrilotriacetic acid coupled single-walled carbon nanotubes for directed self-assembly with polyhistidine-tagged proteins, ***Chem. Mater.***, 20, 1824-1829 (2008)
146. Oka, Y., Omura, M., Kataoka, H. and Touhara, K., Olfactory receptor antagonism between odorants. ***EMBO J.*** 2004, 23, 120-126.
147. Hammond, R. A. and Dube, L., A Systems science perspective and transdisciplinary models for food and

nutrition, ***Proc. Natl. Acad. Sci. U. S. A.*** 109, 12356-12363 (2012)

148. Peri, C., The universe of food quality, ***Food Qual. Prefer.*** 17, 3-8 (2006)
149. Wingerchuk, D. M., Hogancamp, W. F., O'Brien, P. C. and Weinshenker, B. G., The clinical course of neuromyelitis optica (Devic's syndrome), ***Neurology*** 53, 1107-1114 (1999)
150. Wingerchuk, D. M., Lennon, V. A., Pittock, S. J., Lucchinetti, C. F. and Weinshenker, B. G., Revised diagnostic criteria for neuromyelitis optica, ***Neurology*** 66, 1485-1489 (2006)
151. Lennon, V. A., Wingerchuk, D. M., Kryzer, T. J., Pittock, S. J., Lucchinetti, C. F., Fujihara, K., Nakashima, I. and Weinshenker, B. G., A serum autoantibody marker of neuromyelitis optica: distinction from multiple sclerosis, ***Lancet*** 364, 2106-2112 (2004)
152. Lennon, V. A., Kryzer, T. J., Pittock, S. J., Verkman, A. S., Hinson, S. R., IgG marker of optic-spinal multiple sclerosis binds to the aquaporin-4 water channel, ***J. Exp. Med.*** 202, 473-477 (2005)
153. Fazio, R., Malosio, M. L., Lampasona, V., De Feo, D., Privitera, D., Marnetto, F., Centonze, D., Ghezzi, A., Comi, G., Furlan, R. and Martino, G., Antiacquaporin 4 antibodies detection by different techniques in neuromyelitis optica patients, ***Mult. Scler.*** 15, 1153-1163 (2009)
154. Hayakawa, S., Mori, M., Okuta, A., Kamegawa, A., Fujiyoshi, Y., Yoshiyama, Y., Mitsuoka, K., Ishibashi, K., Sasaki, S., Hattori, T. and Kuwabara S., Neuromyelitis optica and anti-aquaporin-4 antibodies measured by an enzyme-linked immunosorbent assay, ***J. Neuroimmunol.*** 196, 181-187 (2008)

155. Jarius, S., Probst, C., Borowski, K., Franciotta, D., Wildemann, B., Stoecker, W. and Wandinger, K. P., Standardized method for the detection of antibodies to aquaporin-4 based on a highly sensitive immunofluorescence assay emplying recombinant target antigen, ***J. Neurol. Sci.*** 291, 52-56 (2010)

156. Marnetto, F., Hellias, B., Granieri, L., Frau, J., Patanella, A. K., Nytrova, P., Sala, A., Capobianco, M., Gilli, F. and Bertolotto, A., Western blot analysis for the detection of serum antibodies recognizing linear Aquaporin-4 epitopes in patients with Neuromyelitis optica, ***J. Neuroimmunol.*** 217, 74-79 (2009)

157. McKeon, A., Fryer, J. P., Apiwattanakul, M., Lennon, V. A., Hinson, S. R., Kryzer, T. J., Lucchinetti, C. F., Weinshenker, B. G., Wingerchuk, D. M., Shuster, E. A.and Pittock, S. J., Diagnosis of neuromyelitis spectrum disorders: comparative sensitivities and specificities of immunohistochemical and immunoprecipitation assays, ***Arch. Neurol.*** 66, 1134-1138 (2009)

158. Paul, F., Jarius, S., Aktas, O., Bluthner, M., Bauer, O., Appelhans, H., Franciotta, D., Bergamaschi, R., Littleton, E., Palace, J., Seelig, H. P., Hohlfeld, R., Vincent, A. and Zipp, F., Antibody to aquaporin 4 in the diagnosis of neuromyelitis optica, ***PLoS Med.*** 4, e133 (2007)

159. Takahashi, T., Fujihara, K., Nakashima, I., Misu, T., Miyazawa, I., Nakamura, M., Watanabe, S., Shiga, Y., Kanaoka, C., Fujimori, J., Sato, S., Itoyama, Y., Anti-aquaporin-4 antibody is involved in the pathogenesis of NMO: a study on antibody titre, ***Brain*** 130, 1235-1243 (2007)

160. Waters, P., Jarius, S., Littleton, E., Leite, M. I., Jacob, S., Gray, B., Geraldes, R., Vale, T., Jacob, A., Palace, J., Maxwell, S., Beeson, D. and Vincent, A., Aquaporin-4 antibodies in neuromyelitis optica and longitudinally extensive transverse myelitis, ***Arch. Neurol.*** 65, 913-919 (2008)

161. Iorio, R., Fryer, J. P., Hinson, S. R., Fallier-Becker, P., Wolburg, H., Pittock, S. J.and Lennon, V. A., Astrocytic autoantibody of neuromyelitis optica (NMO-IgG) binds to aquaporin-4 extracellular loops, monomers, tetramers and high order arrays., ***J. Autoimmun.*** 40, 21-27 (2013)

162. Pisani, F., Mastrototaro, M., Rossi, A., Nicchia, G. P., Tortorella, C., Ruggieri, M., Trojano, M., Frigeri, A. and Svelto, M., Identification of two major conformational aquaporin-4 epitopes for neuromyelitis optica autoantibody binding, ***J. Biol. Chem.*** 286, 9216-9224 (2011)

163. Chen, Y., Li, R., Wu, A. M., Lu, Z. Q. and Hu, X. Q., The complement and immunoglobulin levels in NMO patients, ***Neurol. Sci.***, 2, 215-220 (2014)

164. Lim, J. H., Oh, E. H., Park, J., Hong, S. and Park, T. H., Ion-channel-coupled receptor-based platform for a real-time measurement of G-protein-coupled receptor activities, ***ACS Nano*** 9, 1699-1706 (2015)

165. Cosentino, C. Alberio, L., Gazzarrini, S., Aquila, M., Romano, E., Cermenati, S., Zuccolini, P., Petersen, J., Beltrame, M., Van Etten, J. L., Christie, J. M., Thiel, G. and Moroni, A., Optogenetics. Engineering of a light-gated potassium channel, ***Science*** 348, 707-710 (2015)

166. Yellen, G., The voltage-gated potassium channels and their relatives, ***Nature*** 419, 35-42 (2002

초 록

생체물질을 인지요소로 사용하고 전자장치를 신호변환기로 사용하는 바이오전자 센서는 많은 분야에서 널리 개발되어 왔다. 생물학적 요소에서 영감을 받은 대상물질 검지를 위한 센서의 기능성을 증진시켰다. 나노소자 기반의 전기 장치는 신속히 생체신호를 증폭하여 직관적인 형태로 전환하였다. 더군다나 많은 생물은 활동전위에 의해 작동하여 그 메커니즘이 바이오전자 센서에 적용될 수 있다. 최근 들어 탄소나노튜브, 그래핀, 나노파티클, 나노파이버, 나노필름 등 다양한 나노소자들이 바이오전자 센서 제작에 사용되었다. 이러한 나노소자들은 특이적인 결합을 위해서 DNA, 단백질, 펩타이드, 세포 등의 생체물질과 함께 기능화되었다. 이렇게 제작된 바이오전자 센서들은 낮은 가격, 작은 크기, 빠른 신호, 높은 민감도와 선택도에서 장점이 있다.

본 연구는 탄소나노튜브 기반의 바이오전자 센서를 수용체 단백질과 펩타이드를 이용하여 제작하고 다양한 분야에 적용하는 것에 목적이 있다. 수용체는 세포막 외부의 자극으로 인해 신호전달체계를 활성화 시킨다. 수용체는 인간의 몸 안에서 감각 신호전달, 세포 상호작용, 신경 전달, 호르몬 신호전달 등 중요한 역할을 담당한다. 본 연구에서는 수용체 단백질을 세포 유래의 나노베시클, 정제된 단백질, 합성 펩타이드 형태로 생산하였다. 수용체에 의한 생체신호는 탄소나노튜브 기반의 트랜지스터에 의해 측정되었으며

이는 환경 모니터링, 질병진단, 식품품질평가의 분야에 적용되었다.

후각 수용체의 기능을 확인하기 위해, 이종세포에서의 리포터 유전자 시스템을 이용한 인공 후각 세포를 제작하였다. 바이오마커의 검지를 위한 특이적인 수용체가 선별되었고, 선별된 수용체는 세포막에 발현됨을 확인하였다. 탄소나노튜브로의 신호전달을 위해 인공 세포 유래의 나노베시클을 제작하였다. 탄소나노튜브 기반의 전계 효과 트랜지스터는 전통적인 포토리소그래피 방법으로 제작되었다. 제작된 센서의 탄소나노튜브 채널은 나노베시클로 기능화되었고, 나노베시클 고정화 후에도 센서의 전기적 특성이 유지되었다. 나노베시클 기반의 바이오전자 센서는 대상물질을 높은 민감도와 선택도로 검지하였다. 수용체 단백질을 이용한 바이오전자 센서는 수질 모니터링과 당뇨 진단을 위한 간단하고 신속한 분석 방법으로 활용되었다.

바이오전자 센서의 실용화를 위해서는 다중화 측정 플랫폼의 개발과 소형화된 센서 장치가 필요하다. 네 종류의 수용체 단백질을 대장균에서 발현하고, 정제한 후 계면활성제를 이용하여 마이셀 안에 구조를 재형성하였다. 생산된 단백질들은 다채널 탄소나노튜브 전계 효과 트랜지스터에 고정화되었으며, 센서 채널들은 대상물질들의 동시측정이 가능하도록 디자인되었다. 전류 측정 기기는 제작된 다채널 센서에 맞춤 제작되어 노트북에서 공급되는 전원에 의해 작동되었다. 제작된 센서에서 다양한 물질에 대한 복잡한 패턴인식이 비대상 물질의 간섭 현상 없이 측정 가능하였다. 간단하고 휴대 가능한 바이오전자 기기로 효율적인 식품품질평가

가 가능하였으며 신속한 현장측정 플랫폼으로 활용될 것이 기대되었다.

수용체 단백질 유래의 펩타이드를 리간드 결합 부분의 시퀀스를 기반으로 합성하였다. 펩타이드는 세포막과 같은 주변환경을 필요로 하지 않기 때문에 쉽게 합성이 가능하며 보관이 용이하다. 더군다나 합성된 펩타이드는 말단에 페닐알라닌을 추가하는 간단 방법으로 탄소나노튜브와 파이 상호작용을 이용하여 직접적인 고정화가 가능하다. 수용체 유래의 펩타이드 기반 바이오전자 센서는 시신경 척수염의 혈청 바이오마커를 높은 특이도로 검지하였다. 더군다나, 기존의 측정방법 보다 민감도가 더욱 뛰어나 그 대상의 초기 검출이 가능할 것으로 기대된다.

본 연구에서는 탄소나노튜브와 나노베시클, 단백질, 펩타이드 같은 다양한 유형의 수용체를 이용하여 간단하고 빠르게 바이오마커를 측정하는 방법을 개발하였다. 개발된 센서는 환경 모니터링, 질진단, 식품오염평가에 적용되었으며 휴대 가능한 다중화 측정기기가 사용되었다.

주요어: 바이오전자 센서, 수용체, 탄소나노튜브, 환경 모니터링, 질병 진단, 식품 품질 평가

학 번: 2012-30968